**ENERGY CONVERSION AND MANAGEMENT**

# Design optimization of multi-energy systems using mixed-integer linear programming: Which model complexity and level of detail is sufficient?

Marco Wirtz, Maria Hahn, Thomas Schreiber, Dirk Müller

***RWTH Aachen University**, E.ON Energy Research Center, Institute for Energy Efficient Buildings and Indoor Climate, Mathieustr. 10, Aachen, Germany*

**Please cite journal article:**
https://www.sciencedirect.com/science/article/pii/S0196890421004258

**DOI:** 10.1016/j.enconman.2021.114249

***Accepted manuscript***

# Design optimization of multi-energy systems using mixed-integer linear programming: Which model complexity and level of detail is sufficient?

Marco Wirtz[a,*], Maria Hahn[a], Thomas Schreiber[a], Dirk Müller[a]

[a] *RWTH Aachen University, E.ON Energy Research Center, Institute for Energy Efficient Buildings and Indoor Climate, Mathieustr. 10, Aachen, Germany*

**Abstract**

Designing sustainable, cross-sectoral energy supply systems is a challenging task. A widespread and proven planning approach is mathematical optimization and in particular mixed-integer linear programming (MILP). While numerous MILP models have been presented in literature, there is no convention which level of detail is necessary to obtain reliable energy system designs. In this paper, a systematic performance comparison of 24 MILP models for designing multi-energy systems is conducted. The models include different combinations of five widely used model features: Piece-wise linear investment curves, multiple component resolution, minimum part-load limitations, part-load efficiencies, and start-up costs. The operational performances of the optimal system designs are compared by using a unit commitment optimization with high level of detail. In a district heating case study, the total annualized costs of the unit commitment optimizations differ substantially from 391 to 481 kEUR and the computation times of the design optimizations

*Corresponding author
*Email address:* marco.wirtz@eonerc.rwth-aachen.de (Marco Wirtz)

range from 10 s to more than 10 h. Models that consider part-load efficiencies lead to the lowest system costs but the highest computation times. In addition, simple design heuristics are identified which lead in combination with fast-solving linear models to energy systems with low total annualized costs (410 kEUR, 5 % cost increase).

*Keywords:*
Design optimization, Multi-energy system, MILP, Energy hub, Linear programming, Model complexity

---

## 1. Introduction

In order to reduce carbon emissions and achieve the climate goals formulated in the Paris agreement 2015, a transformation of the energy infrastructure and markets takes place and is driven by the decentralization of energy systems. In order to integrate fluctuating renewable energies and to exploit synergies between different energy sectors (electricity, heating, cooling, and natural gas), multi-energy systems are a promising concept and in the focus of current research [1]. In this field, the concept of energy hubs (EH) is gaining increasing interest for district energy systems [2].

Designing EHs with many different conversion and storage technologies, including renewable energies, is a complex and challenging task [3]. One planning approach that has been developed over the last decades is based on mathematical programming [4]. Especially mixed-integer linear programming (MILP) has proven to be a useful approach within the planning process [5]. In scientific literature, countless MILP models with varying degrees of complexity have been presented [6]: Starting from simple linear models [7],

MILP formulations became more and more complex as modelers strove for higher level of detail and model accuracy. For short-term operation optimization with a small number of time steps, complex models with a large number of operational constraints led to major progress in model accuracy [8]. However, the computational costs of design optimization models with a large number of time steps and binary variables have reached the limit of practical applicability. As a result, bridging the gap between short-term operation models and long-term planning models is a focus of current research [8]. Since the most detailed and complex MILP models cannot be solved within a reasonable time, substantial simplifications are inevitable in state-of-the-art models. However, there is a high degree of uncertainty on how and which MILP models can be simplified without causing any relevant loss of accuracy or reducing the validity of the optimization results. In order to close this gap, a comprehensive analysis of different modeling approaches for MILP models in the field of design optimization is conducted in this paper. The study investigates the impact of different levels of detail for MILPs, regarding model complexity (i.e. computational costs) and the operational performance of the optimal EH design.

### *1.1. Complexity of optimization models*

Investigating model complexity becomes increasingly important since a lot of different calculation models are developed over time but often no conventions exist regarding which level of detail is sufficient to obtain reliable optimization results [9]. The degree of model complexity is limited by computational costs and thus, leads to a trade-off between model accuracy and computing times [10]. In accordance with Ridha et al. [11], the complexity of

a model describes the level of detail with which it represents the real system. The more model features are considered, the more detailed it represents the real system dynamics. However, more complex models do not necessarily lead to more accurate results [12]. Ridha et al. [11] compare 145 energy system models and, in accordance with previous works by Winkelmüller et al. [13] and Senkpiel et al. [14], define four dimensions of complexity:

- Temporal resolution and horizon,
- spatial resolution and horizon,
- mathematical complexity, i.e. model class (linear program (LP), MILP, non-linear) and the approach to cope with uncertainty, and
- system scope, which describes the system components included in the model, and the level of detail of their representation.

The first two dimensions (temporal and spatial resolution) have been investigated in numerous recent studies: Simoes et al. [15] investigate different spatial resolutions of wind and PV generation locations. They find that disaggregating wind generation locations has a significant effect on the results, leading to a lower electricity generation. Kotzur et al. [16] investigate different time series aggregation methods. Results show that representative periods are superior to averaged values and for systems with higher shares of renewables, more representative periods are necessary. Marquant et al. [17] compare modeling approaches with different temporal aggregations (full year representation, design day representation, rolling horizon formulation) with respect to the resulting energy system design and find that aggregation methods do not necessarily lead to a decline of accuracy. Babrowski et

al. [18] propose to split the full range of time steps into multiple smaller subproblems with a smaller number of time steps. They show that the optimization results are consistent with a perfect foresight approach over a full year.

The third complexity dimension (mathematical model class) has also been addressed in recent publications: Ommen et al. [19] compare three different models for operation optimization: An LP, an MILP, and a non-linear model. Substantial differences in the component operation between the models are observed. The MILP is found to be the most appropriate, considering accuracy and runtime. Putz et al. [20] compare an MILP formulation with dynamic programming for solving a unit commitment problem. They find that the dynamic program with state prediction leads to substantially smaller computation times compared to the MILP formulation.

In the field of long-term optimization of national energy systems, the fourth complexity dimension, i.e. the impact of different levels of detail, has been investigated in the following papers: Poncelet et al. [8] investigate whether increasing the temporal resolution or the level of operational detail is more important for the accuracy of the results. They evaluate the operational performance of different energy systems with a detailed unit commitment model. Results show that for systems with low penetration of renewable energies, the impact of both, temporal resolution and level of operational detail, is limited. However, for high penetration of renewables, the impact of the temporal resolution becomes dominant. Based on a case study for Ireland, Welsch et al. [21] find that neglecting detailed operational constraints in the planning models has a strong impact on the optimal capacity mix of

the energy system. Gils et al. [22] compare four mathematical optimization models for the design of national energy systems and find that the representation of individual technologies plays an important role. However, no final conclusions are drawn regarding the degree of detail required for modeling different technologies.

Gabrielli et al. [23] compare different levels of detail for modeling a multi-energy system with different types of fuel cells. They find that neglecting the system dynamics (minimum runtime or ramping limitations) does not significantly affect the optimal system. The least complex model with constant conversion efficiencies, however, results in a substantial accuracy decline.

Zhou et al. [24] find that for a combined cooling, heating and power system the impact of assuming constant efficiencies is small. Due to the installation of multiple CHP units and thermal storages, CHP units can operate close to the nominal power and therefore, the actual efficiencies deviate only slightly from the nominal efficiencies.

Palmintier et al. [25] show that neglecting detailed operational constraints, such as minimum part load, ramping constraints, or operating reserves, leads to a sub-optimal generation portfolio and higher operating costs.

Helistö et al. [26] compare the impact of different temporal resolutions and operational details on investment planning models. They find that for systems with a large share of renewables, sector-coupling technologies should be modeled more detailed and selecting a large number of representative periods becomes more important.

Evins et al. [27] investigate new formulations for increasing the level of detail for EH design models. These comprise minimum runtimes, different

approximations of part-load efficiency curves and storage loss coefficients. They find that increasing the level of operational detail has a substantial effect on the optimal EH design.

In the following, a short summary of MILP formulations for designing EHs is provided and the most relevant modeling features are identified.

### *1.2. Model features*

By analyzing recent publications, the following five model features have been identified as most relevant for EH design models on district scale:

- Piece-wise linear investment curves,
- multiple component resolution,
- minimum part-load limitations,
- part-load efficiencies, and
- start-up costs.

For 29 studies, Table 1 lists which of the five model features are considered in the respective MILP model. While minimum part-load limitations are frequently modeled, piece-wise linear investment curves are usually not considered. In general, no convention exists which combination of model features should be used in design optimization. The following sections introduce the features in more detail and sketch how they are considered in recently published studies.

Table 1: Model features considered (x) in MILP formulations: `I`: Piece-wise linear investment curves, `L`: Minimum part load, `E`: Part-load efficiency, `C`: Multiple component resolution, `S`: Start-up costs.

| Publication | | I | L | E | C | S |
|---|---|---|---|---|---|---|
| Yokoyama et al. (2002) | [28] | x | x | - | - | - |
| Weber et al. (2011) | [29] | x | x | x | - | - |
| Fazlollahi et al. (2012) | [30] | - | x | x | x | - |
| Voll et al. (2012) | [31] | - | x | x | x | - |
| Omu et al. (2013) | [32] | - | x | - | - | - |
| Pruitt et al. (2013) | [33] | - | x | x | - | x |
| Zhou et al. (2013) | [24] | - | x | x | x | - |
| Voll (2014) | [34] | x | x | x | x | - |
| Wakui et al. (2014) | [35] | - | x | x | x | x |
| Bischi et al. (2014) | [36] | - | x | x | - | x |
| Evins et al. (2014) | [27] | - | x | x | - | - |
| Rieder et al. (2014) | [37] | x | x | - | x | - |
| Yokoyama et al. (2015) | [38] | - | x | x | x | - |
| Yang et al. (2015) | [39] | - | x | x | x | - |
| Milan et al. (2015) | [40] | - | x | x | - | - |
| Akbari et al. (2016) | [41] | - | - | - | x | - |
| Morvaj et al. (2016) | [42] | - | x | - | - | x |
| Li et al. (2016) | [43] | - | x | x | - | - |
| Goderbauer et al. (2016) | [44] | - | x | x | x | - |
| Majewski et al. (2017) | [45] | x | x | - | x | - |
| Deng et al. (2017) | [46] | - | x | x | - | - |
| Schütz et al. (2017) | [47] | x | x | x | - | - |
| Sameti et al. (2017) | [5] | - | - | - | x | - |
| Dolatabadi et al. (2017) | [48] | - | x | - | - | x |
| Jing et al. (2018) | [49] | - | x | x | - | x |
| Gonzalez-Castellanos et al. (2018) | [50] | - | x | x | x | x |
| Gabrielli et al. (2018) | [23] | - | x | x | - | - |
| Karmellos et al. (2019) | [51] | - | x | - | - | - |
| Hollermann et al. (2019) | [52] | - | x | - | x | - |

### *1.2.1. Investment curves*

For many technical devices, the relationship between the component's capacity and its investment is non-linear [53]. Generation and storage units with larger capacities have lower specific costs than units with smaller capacities [54]. In MILP models, this non-linearity can be approximated with a piece-wise linear relationship based on manufacturer and literature data [29].

### *1.2.2. Multiple component resolution*

In EHs usually more than one unit of each technology is installed. For instance, if CHP units are installed, usually not only one but multiple small units are used. This modularization increases the robustness of the operation against technical failures, enhances the operational flexibility, and leads to higher efficiencies since multiple smaller units can be operated at higher part loads than one large unit. Modeling multiple components for every technology is a widely used approach: The model by Fazlollahi et al. [30] enables the installation of up to three boilers as well as four gas engines and turbines. Sameti et al. [5] and Yang et al. [39] also model multiple components of every technology. The latter work assumes that all components of a technology have the same capacity.

### *1.2.3. Minimum part load*

Many technical devices cannot operate in arbitrary low part load. Heat generation units like boilers or CHP units usually cannot be operated at loads below 20 % of their nominal capacity. However, the operation of electrical devices, like photovoltaic modules, is often hardly restricted by part-load lim-

itations. As listed in Table 1, minimum part-load limitations are considered in most models.

### *1.2.4. Part-load efficiency*

In models with a low degree of detail, the efficiency of a component is assumed constant over the entire operation range, from full load to minimum part load, for example in [42]. More detailed approaches use non-linear approximations, for example in [44]. A third approach is to use piece-wise linear functions, as published in [55]. A slightly different formulation is presented by Pruitt et al. [33] who define the electrical efficiency as a linear funtion of the relative load (relative load: relation between actual load and capacity). An equivalent formulation is presented in [56].

### *1.2.5. Start-up costs*

Frequent starts and shutdowns of engines can lead to a reduction of their lifetime due to increased wear and tear as well as an increased fuel consumption. These effects can be monetized by introducing specific costs for every component start and/or shutdown. If start-up costs are neglected, the operation of components may be characterized by frequent starts and stops.

In the literature, start-up costs are modeled in different ways: Morvaj et al. [42] and Jing et al. [49] limit the number of starts of CHP units to one per day. Fazlollahi et al. [30] introduce model constraints which ensure that energy conversion units must run a minimum time before they can be shut down. Wakui et al. [35] and Gonzalez-Castellanos et al. [50] penalize start-ups with an increased fuel consumption during start-up intervals. The SIFRE model [55] explicitly considers start-up costs in the objective function

and takes into account the off-time duration before the unit is switched on again. Bischi et al. [36] present a MILP formulation for short-term operation planning of a combined cooling, heat and power system. They penalize every component start with fix costs in the objective function.

### *1.3. Contributions*

A research gap is identified regarding the necessary level of detail in MILP formulations for the design optimization of multi-energy systems. Therefore, in this paper, a systematic comparison of 24 MILP formulations with different levels of detail for the design of EHs on district scale is presented. For this purpose, a base model (linear program) is systematically extended by five widely used model features: Piece-wise linear investment curves, multiple component resolution, minimum part load, part-load efficiencies, and start-up costs. The study aims at answering the following questions:

- How do different model features influence the optimal energy system configuration?
- Which model features are necessary and sufficient to obtain accurate and meaningful optimization results?
- What is the impact of different model features on the computational costs?
- Is it possible to identify models with low complexity that provide as accurate results as the most complex models?

Providing answers to these open questions is highly relevant for future model development in the field of energy system design optimization.

### *1.4. Paper organization*

The paper structure is as follows: In Section 2, the MILP formulations as well as the methods for the comparison and evaluation are described in detail. Based on a case study, the model comparison is conducted in Section 3. The results are generalized and discussed in Section 4. Finally, conclusions and an outlook are provided in Section 5.

## 2. Methods

In this section, the (mixed-integer) linear programs investigated in this study are presented. Firstly, the *base model*, which represents the model with the lowest complexity, is presented in Section 2.1. In Section 2.2, the constraints of the five model features are presented in detail.

### *2.1. Base model (linear program)*

The mathematical optimization model determines the optimal energy supply system to cover time-varying heating and cooling demands. The energy supply system is defined by an optimal selection of energy conversion and storage units, and their optimal sizing. The optimization also models the operation of all system components based on perfect forecasts of demands and weather conditions. Main constraints of the model are energy balances, which ensure that the heating and cooling demands are met in every time step. In this study, the duration of time steps is $\Delta t = 1\,\text{hour}$, which represents a feasible trade-off between accuracy and computational costs [57]. The optimization model is based on design days. For this purpose, the annual time series of heating and cooling demands as well as weather data are

aggregated to 6 design days, using a k-medoids clustering algorithm as presented by Domínguez et al. [58] and implemented by Schütz et al. [57]. In the following formulation, all decision variables of the model are constrained to have non-negative values unless otherwise stated. Decision variables are written in italics while model parameters are written in non-italics. Greek symbols represent model parameters except for $\delta$ and $\xi$, which represent decision variables.

### *2.1.1. Superstructure*

The superstructure of an optimization model comprises all technologies that can be selected in the optimization. The superstructure used in this paper is depicted in Fig. 1: Gas boilers generate heat and PV modules electricity. CHP units are gas-driven and generate heat and electricity. Compression and absorption chillers provide cooling energy. In order to enhance the operational flexibility, batteries as well as heat and cold storages can be selected by the optimization. A connection to the public electricity and gas grid exists.

### *2.1.2. Objective function*

The objective of the optimization is minimizing total annualized costs (TAC). They include annualized investments ($C_{\mathrm{inv}}$), operation and maintenance costs ($C_{\mathrm{om}}$), gas and electricity costs ($C_{\mathrm{gas}}$, $C_{\mathrm{el}}$), and revenues from electricity feed-in ($R_{\mathrm{feed-in}}$):

$$\min TAC = C_{\mathrm{inv}} + C_{\mathrm{om}} + C_{\mathrm{gas}} + C_{\mathrm{el}} - R_{\mathrm{feed-in}} \tag{1}$$

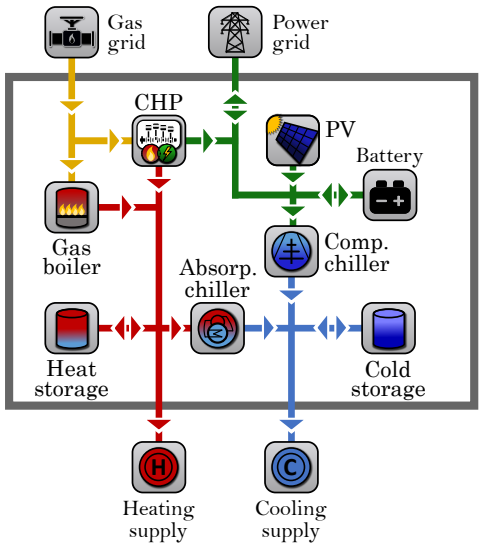


Figure 1: Superstructure of the optimization model with all generation and storage technologies.

For the annualization of investments, an annuity factor $\mathrm{a}_{\mathrm{inv},k}$ is used:

$$C_{\mathrm{inv}} = \sum_{k \in \mathrm{K}} \sum_{m \in \mathrm{M}_k} \mathrm{a}_{\mathrm{inv},k}\, I_{k,m} \tag{2}$$

In the following, $k \in \mathrm{K}$ denotes the technology and $m \in \mathrm{M_k}$ the component (multiple components of the same technology can be selected). The operation and maintenance costs are expressed as a proportion $\mathrm{f}_{\mathrm{om}}$ of the investment costs:

$$C_{\mathrm{om}} = \sum_{k \in \mathrm{K}} \sum_{m \in \mathrm{M}_k} \mathrm{f}_{\mathrm{om},k} I_{k,m} \tag{3}$$

All technical and economic model parameters are listed in Appendix A. The investment $I$ is modeled with constant specific investments i:

$$I_{k,m} = \mathrm{i}_k cap_{k,m} \quad \forall \;\; k \in \mathrm{K}, \quad m \in \mathrm{M}_k \tag{4}$$

Here, $cap_{k,m}$ denotes the nominal power of each component. For gas boilers, compression and absorption chillers, *cap* denotes the rated heating and cooling power. For CHP units and PV installations, it denotes the rated electric power. For energy storages, *cap* represents the storage capacity.

The gas costs result from the total amount of gas purchased ($G_{\mathrm{grid,tot}}$) and the gas price ($\mathrm{p_{gas}}$):

$$C_{\mathrm{gas}} = G_{\mathrm{grid,tot}}\ \mathrm{p_{gas}} \tag{5}$$

The total gas demand of the system is obtained by summing up the gas demand for all time steps $t$ of all design days $d$:

$$G_{\mathrm{grid,tot}} = \sum_{d \in \mathrm{D}} \mathrm{w}_d \sum_{t \in \mathrm{T}} \left( \sum_{m \in \mathrm{M_{BOI}}} \dot{G}_{\mathrm{BOI},m,d,t} + \sum_{m \in \mathrm{M_{CHP}}} \dot{G}_{\mathrm{CHP},m,d,t} \right) \Delta \mathrm{t} \tag{6}$$

$\mathrm{w}_d$ describes the number of days of a year which design day $d$ represents. The electricity costs are captured by:

$$C_{\mathrm{el}} = \sum_{d \in \mathrm{D}} \mathrm{w}_d \sum_{t \in \mathrm{T}} P_{\mathrm{grid},d,t}\ \mathrm{p_{el},}_{d,t} \Delta \mathrm{t} \tag{7}$$

Here, $\mathrm{p_{el},}_{d,t}$ denotes the electricity price and $P_{\mathrm{grid},d,t}$ the power import from the grid.

Feed-in revenues result from excess power of CHP units and PV:

$$R^{\mathrm{feed-in}} = R^{\mathrm{feed-in}}_{\mathrm{CHP}} + R^{\mathrm{feed-in}}_{\mathrm{PV}} \tag{8}$$

with the revenues for each technology as follows:

$$R^{\mathrm{feed-in}}_{\mathrm{CHP}} = \sum_{d \in \mathrm{D}} \mathrm{w}_d \sum_{t \in \mathrm{T}} \left( \sum_{m \in \mathrm{M_{CHP}}} P_{\mathrm{feed-in,CHP},d,t}\ \mathrm{r_{feed-in,CHP},}_{d,t} \right) \Delta \mathrm{t} \tag{9}$$

$$R^{\mathrm{feed-in}}_{\mathrm{PV}} = \sum_{d \in \mathrm{D}} \mathrm{w}_d \sum_{t \in \mathrm{T}} \left( P_{\mathrm{feed-in,PV},d,t}\ \mathrm{r_{feed-in,PV},}_{d,t} \right) \Delta \mathrm{t} \tag{10}$$

*2.1.3. Constraints*

In the following, the optimization constraints of the base model are described in detail.

**Technologies**

The nominal capacity of all components, except for the PV modules, is a free positive variable. The PV area is limited by the maximum available area:

$$A_{\mathrm{PV}} \leq \mathrm{A}_{\mathrm{PV}}^{\mathrm{max}} \tag{11}$$

The rated PV power (under Standard Test Conditions (STC) [59]) is

$$P_{\mathrm{PV}}^{\mathrm{nom}} = \mathrm{G}_{\mathrm{sol,STC}} A_{\mathrm{PV}}\, \eta_{\mathrm{PV,STC}} \tag{12}$$

Here, $\mathrm{G}_{\mathrm{sol,STC}}$ is the global irradiance and $\eta_{\mathrm{PV,STC}}$ the electric efficiency under Standard Test Conditions.

The power of all components is limited by their nominal power:

$$\dot{Q}_{\mathrm{h,BOI},m,d,t} \leq \dot{Q}_{\mathrm{h,BOI},m}^{\mathrm{nom}} \quad \forall\, m \in \mathrm{M_{BOI}}, \quad d \in \mathrm{D}, \quad t \in \mathrm{T} \tag{13}$$

$$\dot{Q}_{\mathrm{c,CC},m,d,t} \leq \dot{Q}_{\mathrm{c,CC},m}^{\mathrm{nom}} \quad \forall\, m \in \mathrm{M_{CC}}, \quad d \in \mathrm{D}, \quad t \in \mathrm{T} \tag{14}$$

$$\dot{Q}_{\mathrm{c,AC},m,d,t} \leq \dot{Q}_{\mathrm{c,AC},m}^{\mathrm{nom}} \quad \forall\, m \in \mathrm{M_{AC}}, \quad d \in \mathrm{D}, \quad t \in \mathrm{T} \tag{15}$$

$$P_{\mathrm{CHP},m,d,t} \leq P_{\mathrm{CHP},m}^{\mathrm{nom}} \quad \forall\, m \in \mathrm{M_{CHP}}, \quad d \in \mathrm{D}, \quad t \in \mathrm{T} \tag{16}$$

$$P_{\mathrm{PV},d,t} \leq P_{\mathrm{PV}}^{\mathrm{nom}} \quad \forall\, d \in \mathrm{D}, \quad t \in \mathrm{T} \tag{17}$$

Here, $\dot{Q}_{\mathrm{h},k,m}^{\mathrm{nom}}$, $\dot{Q}_{\mathrm{c},k,m}^{\mathrm{nom}}$, and $P_{k,m}^{\mathrm{nom}}$ denote the rated heating, cooling and electric power of component $m$ and technology $k$, respectively. $\dot{Q}_{\mathrm{h},k,m,d,t}$, $\dot{Q}_{\mathrm{c},k,m,d,t}$, and $P_{k,m,d,t}$ denote the heating, cooling, and electric power at time step $t$ and design day $d$, respectively. The thermal power of gas boilers, compression

and absorption chillers are expressed with their thermal efficiencies:

$$\dot{Q}_{\mathrm{h,BOI},m,d,t} = \dot{G}_{\mathrm{BOI},m,d,t}\, \eta^{\mathrm{nom}}_{\mathrm{BOI}} \quad \forall \;\; m \in \mathrm{M_{BOI}}, \quad d \in \mathrm{D}, \quad t \in \mathrm{T} \tag{18}$$

$$\dot{Q}_{\mathrm{c,CC},m,d,t} = P_{\mathrm{CC},m,d,t}\, \mathrm{COP}^{\mathrm{nom}}_{\mathrm{CC}} \quad \forall \;\; m \in \mathrm{M_{CC}}, \quad d \in \mathrm{D}, \quad t \in \mathrm{T} \tag{19}$$

$$\dot{Q}_{\mathrm{c,AC},m,d,t} = \dot{Q}_{\mathrm{h,AC},m,d,t}\, \beta^{\mathrm{nom}}_{\mathrm{AC}} \quad \forall \;\; m \in \mathrm{M_{AC}}, \quad d \in \mathrm{D}, \quad t \in \mathrm{T} \tag{20}$$

Here, $\dot{Q}_{\mathrm{h,AC,m},d,t}$ denotes the heat flow that drives the absorption chiller and $\dot{Q}_{\mathrm{c,AC,m},d,t}$ its cooling power. The thermal efficiency of gas boilers, the heat ratio of absorption chillers, and the coefficient of performance (COP) of compression chillers are assumed constant.

Constant thermal and electric efficiencies are assumed for CHP units:

$$P_{\mathrm{CHP},m,d,t} = \dot{G}_{\mathrm{CHP},m,d,t}\, \eta^{\mathrm{nom}}_{\mathrm{el,CHP}} \quad \forall \;\; m \in \mathrm{M_{CHP}}, \quad d \in \mathrm{D}, \quad t \in \mathrm{T} \tag{21}$$

$$\dot{Q}_{\mathrm{h,CHP},m,d,t} = \dot{G}_{\mathrm{CHP},m,d,t}\, \eta^{\mathrm{nom}}_{\mathrm{th,CHP}} \quad \forall \;\; m \in \mathrm{M_{CHP}}, \quad d \in \mathrm{D}, \quad t \in \mathrm{T} \tag{22}$$

The power of the PV modules is expressed with the global tilted irradiance ($\mathrm{G}_{\mathrm{sol},d,t}$) and the module efficiency ($\eta_{\mathrm{PV},d,t}$), which depends on the ambient air temperature and is calculated in a pre-processing step:

$$P_{\mathrm{PV},d,t} \leq \mathrm{G}_{\mathrm{sol},d,t} A_{\mathrm{PV}}\, \eta_{\mathrm{PV},d,t} \quad \forall \;\; d \in \mathrm{D}, \quad t \in \mathrm{T} \tag{23}$$

The inequality enables curtailment of PV power.

**Energy storages**

Thermal and electric storages are modeled according to a formulation by Gabrielli et al. [60] and Kotzur et al. [61], which allows a seasonal operation of storages, despite using design days. The state of charge $S_{k,m,n,t}$ of each component of storage technology $k \in \mathrm{K_{sto}}$ (battery, heat, and cold storage)

for each day of the year $n \in \mathrm{N_{year}}$ with $\mathrm{N_{year}} = \{1, 2, ..., 365\}$ is:

$$S_{k,m,n,t} = S_{k,m,n,t-1}\,(1 - \phi_{k,\mathrm{loss}}) + \eta_k^{\mathrm{ch}} P_{k,m,\sigma(n),t}^{\mathrm{ch}} - \frac{P_{k,m,\sigma(n),t}^{\mathrm{dch}}}{\eta_k^{\mathrm{dch}}}$$
$$\forall \;\; k \in \mathrm{K_{sto}}, \quad m \in \mathrm{M}_k, \quad n \in \mathrm{N_{year}}, \quad t \in \mathrm{T} : \; t \neq 1 \tag{24}$$

Here, $\phi_{k,\mathrm{loss}}$ is a stand-by loss coefficient (for thermal storages 0.5 %/h, for batteries 0.1 %/h). $\eta_k^{\mathrm{ch}}$ and $\eta_k^{\mathrm{dch}}$ denote charging and discharging efficiencies (for batteries 0.96, for thermal storages 1). The function $\sigma$ describes the assignment between all days of the year $n$ and design days $d$:

$$\sigma : \mathrm{N_{year}} \rightarrow \mathrm{D}, \; \sigma(n) = d \tag{25}$$

$P^{\mathrm{ch}}$ and $P^{\mathrm{dch}}$ denote charging and discharging energy flows. The first time step of day $n$ is connected to the 24th time step of the previous day $(n-1)$:

$$S_{k,m,n,1} = S_{k,m,n-1,24}\,(1 - \phi_{k,\mathrm{loss}}) + \eta_k^{\mathrm{ch}} P_{k,m,\sigma(n),1}^{\mathrm{ch}} - \frac{P_{k,m,\sigma(n),1}^{\mathrm{dch}}}{\eta_k^{\mathrm{dch}}}$$
$$\forall \;\; k \in \mathrm{K_{sto}}, \quad m \in \mathrm{M}_k, \quad n \in \mathrm{N_{year}} : \; n \neq 1 \tag{26}$$

The first time step of the first day is connected to the 24th time step of the 365th day (cyclic condition):

$$S_{k,m,1,1} = S_{k,m,365,24}\,(1 - \phi_{k,\mathrm{loss}}) + \eta_k^{\mathrm{ch}} P_{k,m,\sigma(1),1}^{\mathrm{ch}} - \frac{P_{k,m,\sigma(1),1}^{\mathrm{dch}}}{\eta_k^{\mathrm{dch}}}$$
$$\forall \;\; k \in \mathrm{K_{sto}}, \quad m \in \mathrm{M}_k \tag{27}$$

The state of charge is limited by a minimum and maximum proportion of the capacity (for batteries $\mathrm{s}_k^{\min} = 0.2$ and $\mathrm{s}_k^{\max} = 0.8$):

$$S_{k,m,n,t} \leq \mathrm{s}_k^{\max} S_{k,m}^{\mathrm{cap}} \quad \forall \;\; k \in \mathrm{K_{sto}}, \quad m \in \mathrm{M}_k, \quad n \in \mathrm{N_{year}}, \quad t \in \mathrm{T} \tag{28}$$

$$S_{k,m,n,t} \geq \mathrm{s}_k^{\min} S_{k,m}^{\mathrm{cap}} \quad \forall \;\; k \in \mathrm{K_{sto}}, \quad m \in \mathrm{M}_k, \quad n \in \mathrm{N_{year}}, \quad t \in \mathrm{T} \tag{29}$$

A minimum charging and discharging time $\tau$ (for batteries: 3 h, for thermal storages: 4 h) limits the charging and discharging power:

$$P^{\mathrm{ch}}_{k,m,d,t} \leq \frac{S^{\mathrm{cap}}_{k,m}}{\tau_k} \quad \forall \;\; k \in \mathrm{K_{sto}}, \quad m \in \mathrm{M}_k, \quad d \in \mathrm{D}, \quad t \in \mathrm{T} \tag{30}$$

$$P^{\mathrm{dch}}_{k,m,d,t} \leq \frac{S^{\mathrm{cap}}_{k,m}}{\tau_k} \quad \forall \;\; k \in \mathrm{K_{sto}}, \quad m \in \mathrm{M}_k, \quad d \in \mathrm{D}, \quad t \in \mathrm{T} \tag{31}$$

**Energy balances**

Three energy balances ensure that all heating and cooling demands are covered by the EH. The heat balance is

$$\begin{aligned} &\sum_{m \in \mathrm{M_{BOI}}} \dot{Q}_{\mathrm{h,BOI},m,d,t} + \sum_{m \in \mathrm{M_{CHP}}} \dot{Q}_{\mathrm{h,CHP},m,d,t} + \sum_{m \in \mathrm{M_{TES}}} \dot{Q}^{\mathrm{dch}}_{\mathrm{h,TES},m,d,t} \\ &= \dot{Q}_{\mathrm{h,dem},d,t} + \sum_{m \in \mathrm{M_{AC}}} \dot{Q}_{\mathrm{h,AC},m,d,t} + \sum_{m \in \mathrm{M_{TES}}} \dot{Q}^{\mathrm{ch}}_{\mathrm{h,TES},m,d,t} \quad \forall \;\; d \in \mathrm{D}, \quad t \in \mathrm{T} \end{aligned} \tag{32}$$

which includes the heat flows from and to all components (boilers, CHP units, charging and discharging of heat storages, absorption chillers, and the demand of the district heating network). The cold balance comprises the cold generation of the chillers, the cold storage, and the demand of the cooling network:

$$\begin{aligned} &\sum_{m \in \mathrm{M_{CC}}} \dot{Q}_{\mathrm{c,CC},m,d,t} + \sum_{m \in \mathrm{M_{AC}}} \dot{Q}_{\mathrm{c,AC},m,d,t} + \sum_{m \in \mathrm{M_{CTES}}} \dot{Q}^{\mathrm{dch}}_{\mathrm{c,CTES},m,d,t} \\ &= \dot{Q}_{\mathrm{c,dem},d,t} + \sum_{m \in \mathrm{M_{CTES}}} \dot{Q}^{\mathrm{ch}}_{\mathrm{c,CTES},m,d,t} \quad \forall \;\; d \in \mathrm{D}, \quad t \in \mathrm{T} \end{aligned} \tag{33}$$

The electric power balance includes power generation by CHP units and PV modules, electricity import from and export to the grid as well as charging

and discharging flows from and to the battery:

$$\sum_{m \in \mathrm{M_{CHP}}} P_{\mathrm{CHP},m,d,t} + P_{\mathrm{PV},d,t} + \sum_{m \in \mathrm{M_{BAT}}} P^{\mathrm{dch}}_{\mathrm{BAT},m,d,t} + P_{\mathrm{grid},d,t}$$
$$= \sum_{m \in \mathrm{M_{CC}}} P_{\mathrm{CC},m,d,t} + \sum_{m \in \mathrm{M_{BAT}}} P^{\mathrm{ch}}_{\mathrm{BAT},m,d,t} + P_{\mathrm{feed-in},d,t} \quad \forall \ d \in \mathrm{D}, \quad t \in \mathrm{T} \quad (34)$$

Feed-in power results from CHP units, PV modules, or batteries:

$$P_{\mathrm{feed-in},d,t} = \sum_{m \in \mathrm{M_{CHP}}} P_{\mathrm{feed-in,CHP},d,t} + P_{\mathrm{feed-in,PV},d,t} \quad \forall \ d \in \mathrm{D}, \quad t \in \mathrm{T} \quad (35)$$

$$\sum_{m \in \mathrm{M_{CHP}}} P_{\mathrm{feed-in,CHP},d,t} \leq \sum_{m \in \mathrm{M_{CHP}}} P_{\mathrm{CHP},m,d,t} + \sum_{m \in \mathrm{M_{BAT}}} P^{\mathrm{dch}}_{\mathrm{BAT},m,d,t} \quad (36)$$

$$P_{\mathrm{feed-in,PV},d,t} \leq P_{\mathrm{PV},d,t} \quad (37)$$

Due to the design day clustering, the peak demands of the clustered demand time series are not necessarily equal to the peak demands of the unclustered demand time series ($\dot{Q}^{\mathrm{max}}_{\mathrm{h,dem}}$, $\dot{Q}^{\mathrm{max}}_{\mathrm{c,dem}}$). In order to avoid undersizing of the generation units, the following constraints ensure that the peak demands of the unclustered demand time series can be covered:

$$\sum_{m \in \mathrm{M_{CHP}}} P^{\mathrm{nom}}_{\mathrm{CHP},m} \frac{\eta^{\mathrm{nom}}_{\mathrm{th,CHP}}}{\eta^{\mathrm{nom}}_{\mathrm{el,CHP}}} + \sum_{m \in \mathrm{M_{BOI}}} \dot{Q}^{\mathrm{nom}}_{\mathrm{h,BOI},m} \geq \dot{Q}^{\mathrm{max}}_{\mathrm{h,dem}} \quad (38)$$

$$\sum_{m \in \mathrm{M_{CC}}} \dot{Q}^{\mathrm{nom}}_{\mathrm{c,CC},m} + \sum_{m \in \mathrm{M_{AC}}} \dot{Q}^{\mathrm{nom}}_{\mathrm{c,AC},m} \geq \dot{Q}^{\mathrm{max}}_{\mathrm{c,dem}} \quad (39)$$

The base model presented in this section is an LP. The modifications to the base model are described for each model feature in the following section.

### *2.2. Model features*

For the features minimum part load, part-load efficiencies as well as start-up costs, the binary variable $y_{k,m,d,t}$ is introduced which makes the model an

MILP. This binary variable indicates if a component $m$ of a technology $k$ is running at a certain time step ($y_{k,m,d,t} = 1$) or not ($y_{k,m,d,t} = 0$). The following big-M constraints ensure that the power of a component is zero if and only if the respective binary variable $y$ is zero:

$$\dot{Q}_{\mathrm{h,BOI},m,d,t} \leq y_{\mathrm{BOI},m,d,t}\hat{\mathrm{M}} \quad \forall \ m \in \mathrm{M_{BOI}}, \quad d \in \mathrm{D}, \quad t \in \mathrm{T} \tag{40}$$

$$y_{\mathrm{BOI},m,d,t} \leq \dot{Q}_{\mathrm{h,BOI},m,d,t}\hat{\mathrm{M}} \quad \forall \ m \in \mathrm{M_{BOI}}, \quad d \in \mathrm{D}, \quad t \in \mathrm{T} \tag{41}$$

$$\dot{Q}_{\mathrm{c},k,m,d,t} \leq y_{k,m,d,t}\hat{\mathrm{M}} \quad \forall \ k \in \{\mathrm{CC}, \mathrm{AC}\}, \quad m \in \mathrm{M}_k, \quad d \in \mathrm{D}, \quad t \in \mathrm{T} \tag{42}$$

$$y_{k,m,d,t} \leq \dot{Q}_{\mathrm{c},k,m,d,t}\hat{\mathrm{M}} \quad \forall \ k \in \{\mathrm{CC}, \mathrm{AC}\}, \quad m \in \mathrm{M}_k, \quad d \in \mathrm{D}, \quad t \in \mathrm{T} \tag{43}$$

$$P_{\mathrm{CHP},m,d,t} \leq y_{\mathrm{CHP},m,d,t}\hat{\mathrm{M}} \quad \forall \ m \in \mathrm{M_{CHP}}, \quad d \in \mathrm{D}, \quad t \in \mathrm{T} \tag{44}$$

$$y_{\mathrm{CHP},m,d,t} \leq P_{\mathrm{CHP},m,d,t}\hat{\mathrm{M}} \quad \forall \ m \in \mathrm{M_{CHP}}, \quad d \in \mathrm{D}, \quad t \in \mathrm{T} \tag{45}$$

*2.2.1. Piece-wise linear investments*

Piece-wise linear investment curves are used to take into account that generation and storage units with high capacity have lower specific costs than units with lower capacity. For modeling piece-wise linear investment curves, auxiliary variables $\xi_{k,m,i}$ for each technology $k$ and each supporting point $i \in \mathrm{N}_k$ are introduced. The auxiliary variables couple the investment costs with the nominal power of the component:

$$\dot{Q}^{\mathrm{nom}}_{\mathrm{h,BOI},m} = \sum_{i \in \mathrm{N_{BOI}}} \xi_{\mathrm{BOI},m,i} \dot{\mathrm{Q}}^{\mathrm{nom}}_{\mathrm{h,BOI},m,i} \quad \forall \ m \in \mathrm{M_{BOI}} \tag{46}$$

$$\dot{Q}^{\mathrm{nom}}_{\mathrm{c},k,m} = \sum_{i \in \mathrm{N}_k} \xi_{k,m,i} \dot{\mathrm{Q}}^{\mathrm{nom}}_{\mathrm{c},k,i} \quad \forall \ m \in \mathrm{M_k}, \quad k \in \{\mathrm{CC}, \mathrm{AC}\} \tag{47}$$

$$P^{\mathrm{nom}}_{\mathrm{CHP},m} = \sum_{i \in \mathrm{N_{CHP}}} \xi_{\mathrm{CHP},m,i} \mathrm{P}^{\mathrm{nom}}_{\mathrm{CHP},m,i} \quad \forall \ m \in \mathrm{M_{CHP}} \tag{48}$$

$$S^{\mathrm{cap}}_{k,m} = \sum_{i \in \mathrm{N}_k} \xi_{k,m,i} \mathrm{S}^{\mathrm{cap}}_{k,m,i} \quad \forall \ m \in \mathrm{M_k}, \quad k \in \{\mathrm{TES}, \mathrm{CTES}\} \tag{49}$$

For each component, a Special Ordered Set 2 (SOS2) is introduced, which ensures that at most two neighboring $\xi_{k,m,i}$ in the SOS2 are greater than zero. In addition, the sum of all auxiliary variables must equal 1:

$$\sum_{i \in \mathrm{N}_k} \xi_{k,m,i} = 1 \quad \forall \quad m \in \mathrm{M}_k, \quad k \in \{\mathrm{BOI}, \mathrm{CC}, \mathrm{AC}, \mathrm{CHP}, \mathrm{TES}, \mathrm{CTES}\} \tag{50}$$

For the technologies PV and battery, the investment curve is in accurate approximation linear due to their modular installation structure. The raw data used in this study as well as the linear and piece-wise linear investment curves are depicted in the Appendix (Fig. A.11 – A.15).

*2.2.2. Component resolution*

The feature of having multiple components of the same technology is realized by setting the cardinality of the component to a value larger than 1. In this study, a maximum of 3 components is considered for each technology:

$$|\mathrm{M}_k| = 3 \quad \forall \quad k \in \{\mathrm{BOI}, \mathrm{CC}, \mathrm{AC}, \mathrm{CHP}, \mathrm{TES}, \mathrm{CTES}, \mathrm{BAT}\} \tag{51}$$

If only the feature *component resolution* is enabled, the optimization model remains an LP. In this specific case, arbitrarily many optimal solutions exist which all have the same objective value. This is because the distribution of the total capacity of a technology to the components has no effect in the design model. For example, a solution with 3 boilers with 1 MW each has the same objective value as installing only 1 boiler with 3 MW capacity. Since this choice is therefore random and does not add any meaningful insights, further constraints are introduced in this special case, which ensure that the components' capacity of each technology is equal:

$$cap_{k,1} = cap_{k,2} = cap_{k,3} \quad \forall \quad k \in \mathrm{K} \tag{52}$$

Table 2: Minimum part-load ratios [51, 52, 43]

| Technology | Part-load ratio |
|---|---|
| Gas boiler | 0.2 |
| CHP unit | 0.5 |
| Compression chiller | 0.2 |
| Absorption chiller | 0.2 |

This means, a total capacity of 3 MW is split into three components of 1 MW.

*2.2.3. Minimum part load*

The operation of thermal energy conversion units is usually limited by a minimum part-load ratio (PLR) which is modeled by the following constraints:

$$\mathrm{PLR}_{\mathrm{BOI}} \dot{Q}^{\mathrm{nom}}_{\mathrm{h,BOI},m} \leq \dot{Q}_{\mathrm{h,BOI},m,d,t} + \hat{\mathrm{M}}(1 - y_{\mathrm{BOI},m,d,t}) \quad \forall \;\; m \in \mathrm{M}_{\mathrm{BOI}}, \;\; d \in \mathrm{D}, \;\; t \in \mathrm{T} \tag{53}$$

$$\mathrm{PLR}_{m} \dot{Q}^{\mathrm{nom}}_{\mathrm{c},k,m} \leq \dot{Q}_{\mathrm{c},k,m,d,t} + \hat{\mathrm{M}}(1 - y_{k,m,d,t}) \quad \forall \;\; k \in \{\mathrm{CC}, \mathrm{AC}\}, \;\; m \in \mathrm{M}_{k}, \;\; d \in \mathrm{D}, \;\; t \in \mathrm{T} \tag{54}$$

$$\mathrm{PLR}_{\mathrm{CHP}} P^{\mathrm{nom}}_{\mathrm{CHP},m} \leq P_{\mathrm{CHP},m,d,t} + \hat{\mathrm{M}}(1 - y_{\mathrm{CHP},m,d,t}) \quad \forall \;\; m \in \mathrm{M}_{\mathrm{CHP}}, \;\; d \in \mathrm{D}, \;\; t \in \mathrm{T} \tag{55}$$

Here, a big-M formulation is used in accordance with recent literature [42]. Minimum part-load ratios used in this investigation are listed in Table 2. Part-load restrictions are neglected for PV modules.

*2.2.4. Part-load efficiency*

In this study, part-load efficencies are considered for gas boilers, CHP units, compression and absorption chillers. The formulation is adapted from [34]. No part-load decline of PV modules is taken into account. The non-linear efficiency curves used in this study are illustrated in Fig. 2 and listed in Tables A.9 – A.12 of the Appendix.

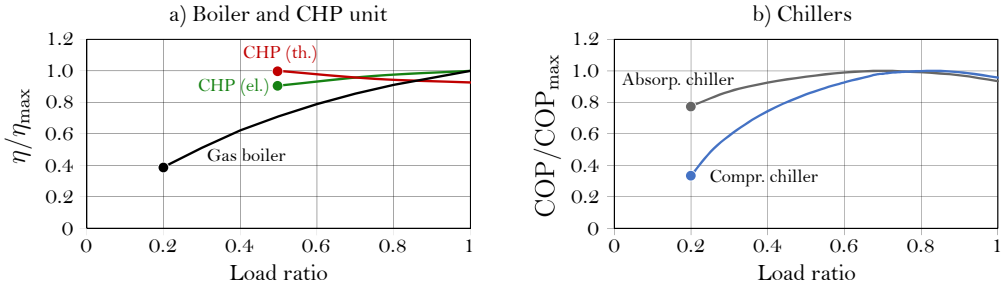


Figure 2: Normalized efficiencies for a) gas boiler and CHP unit and b) compression and absorption chiller.

In order to model part-load efficiencies, a formulation published in [34] is adapted, which results in the following constraints ($\forall\ d \in \mathrm{D},\ t \in \mathrm{T}$):

$$\dot{G}_{\mathrm{BOI},m,d,t} = \dot{Q}^{\mathrm{nom,aux}}_{\mathrm{h,BOI},m,d,t}\gamma_{\mathrm{BOI}} + \dot{Q}_{\mathrm{h,BOI},m,d,t}\lambda_{\mathrm{BOI}} \quad \forall\ m \in \mathrm{M_{BOI}} \tag{56}$$

$$\dot{G}_{\mathrm{CHP},m,d,t} = P^{\mathrm{nom,aux}}_{\mathrm{CHP},m,d,t}\gamma_{\mathrm{el,CHP}} + P_{\mathrm{CHP},m,d,t}\lambda_{\mathrm{el,CHP}} \quad \forall\ m \in \mathrm{M_{CHP}} \tag{57}$$

$$\dot{Q}_{\mathrm{h,CHP},m,d,t} = P^{\mathrm{nom,aux}}_{\mathrm{CHP},m,d,t}\gamma_{\mathrm{th,CHP}} + P_{\mathrm{CHP},m,d,t}\lambda_{\mathrm{th,CHP}} \quad \forall\ m \in \mathrm{M_{CHP}} \tag{58}$$

$$P_{\mathrm{CC},m,d,t} = \dot{Q}^{\mathrm{nom,aux}}_{\mathrm{c,CC},m,d,t}\gamma_{\mathrm{CC}} + \dot{Q}_{\mathrm{c,CC},m,d,t}\lambda_{\mathrm{CC}} \quad \forall\ m \in \mathrm{M_{CC}} \tag{59}$$

$$\dot{Q}_{\mathrm{h,AC},m,d,t} = \dot{Q}^{\mathrm{nom,aux}}_{\mathrm{c,AC},m,d,t}\gamma_{\mathrm{AC}} + \dot{Q}_{\mathrm{c,AC},m,d,t}\lambda_{\mathrm{AC}} \quad \forall\ m \in \mathrm{M_{AC}} \tag{60}$$

Here, the power input of a component (e.g. gas demand of gas boiler) is expressed by the power output (e.g. heat generated by gas boiler), an auxiliary variable ($P^{\mathrm{nom,aux}}/\dot{Q}^{\mathrm{nom,aux}}$) and two linearization parameters $\gamma$ and $\lambda$. The

linearization parameters are fitted with the non-linear efficiency curves and listed for all technologies in Table A.8 of the Appendix.

The auxiliary variables $P^{\mathrm{nom,aux}}$ and $\dot{Q}^{\mathrm{nom,aux}}$ are the product of rated power and binary variable $y$. This means, the auxiliary variable equals the nominal power of the component if the component is running (y=1) otherwise the auxiliary variable is zero. The product of the auxiliary variable and binary variable is linearized by the following reformulation ($\forall\ d \in \mathrm{D},\ t \in \mathrm{T}$):

$$\dot{Q}^{\mathrm{nom,aux}}_{\mathrm{h,BOI},m,d,t} \leq y_{\mathrm{BOI},m,d,t}\hat{\mathrm{M}} \quad \forall\ \ m \in \mathrm{M_{BOI}} \tag{61}$$

$$\dot{Q}^{\mathrm{nom,aux}}_{\mathrm{h,BOI},m,d,t} \leq \dot{Q}^{\mathrm{nom}}_{\mathrm{h,BOI},m} \quad \forall\ \ m \in \mathrm{M_{BOI}} \tag{62}$$

$$\dot{Q}^{\mathrm{nom}}_{\mathrm{h,BOI},m} - (1 - y_{\mathrm{BOI},m,d,t})\hat{\mathrm{M}} \leq \dot{Q}^{\mathrm{nom,aux}}_{\mathrm{h,BOI},m,d,t} \quad \forall\ \ m \in \mathrm{M_{BOI}} \tag{63}$$

$$P^{\mathrm{nom,aux}}_{\mathrm{CHP},m,d,t} \leq y_{\mathrm{CHP},m,d,t}\hat{\mathrm{M}} \quad \forall\ \ m \in \mathrm{M_{CHP}} \tag{64}$$

$$P^{\mathrm{nom,aux}}_{\mathrm{CHP},m,d,t} \leq P^{\mathrm{nom}}_{\mathrm{CHP},m} \quad \forall\ \ m \in \mathrm{M_{CHP}} \tag{65}$$

$$P^{\mathrm{nom}}_{\mathrm{CHP},m} - (1 - y_{\mathrm{CHP},m,d,t})\hat{\mathrm{M}} \leq P^{\mathrm{nom,aux}}_{\mathrm{CHP},m,d,t} \quad \forall\ \ m \in \mathrm{M_{CHP}} \tag{66}$$

$$\dot{Q}^{\mathrm{nom,aux}}_{\mathrm{c},k,m,d,t} \leq y_{k,m,d,t}\hat{\mathrm{M}} \quad \forall\ \ k \in \{\mathrm{CC},\mathrm{AC}\},\ \ m \in \mathrm{M}_k \tag{67}$$

$$\dot{Q}^{\mathrm{nom,aux}}_{\mathrm{c},k,m,d,t} \leq \dot{Q}^{\mathrm{nom}}_{\mathrm{c},k,m} \quad \forall\ \ k \in \{\mathrm{CC},\mathrm{AC}\},\ \ m \in \mathrm{M}_k \tag{68}$$

$$\dot{Q}^{\mathrm{nom}}_{\mathrm{c},k,m} - (1 - y_{k,m,d,t})\hat{\mathrm{M}} \leq \dot{Q}^{\mathrm{nom,aux}}_{\mathrm{c},k,m,d,t} \quad \forall\ \ k \in \{\mathrm{CC},\mathrm{AC}\},\ \ m \in \mathrm{M}_k \tag{69}$$

The linearization errors are visualized in Fig. A.16 of the Appendix.

*2.2.5. Start-up costs*

In order to take into account start-up costs, the objective function is extended by the summand $C_{\mathrm{starts}}$:

$$\min TAC = C_{\mathrm{inv}} + C_{\mathrm{om}} + C_{\mathrm{gas}} + C_{\mathrm{el}} - R_{\mathrm{feed-in}} + C_{\mathrm{starts}} \tag{70}$$

In this study, the modeling approach by Bischi et al. [36] is used to consider start-up costs for CHP units and compression chillers. For these

technologies, frequent start-ups are particularly damaging, as the moving mechanical parts are stressed and worn during start-ups and shutdowns.

For modeling start-up costs, a set of binary variables $\delta^{\text{day}}_{k,m,d,t}$ is introduced, which indicates if a component is switched on during the respective time interval ($\delta = 1$) or not ($\delta = 0$). With the operation variables $y$, this is formulated for all $d \in \mathrm{D},\ t \in \mathrm{T}:\ t \neq 1$ as follows:

$$\delta^{\text{day}}_{k,m,d,t} \geq y_{k,m,d,t} - y_{k,m,d,t-1} \quad \forall\ k \in \{\mathrm{CHP}, \mathrm{CC}\}, \quad m \in \mathrm{M}_k \tag{71}$$

$$\delta^{\text{day}}_{k,m,d,t} \leq 1 - y_{k,m,d,t-1} \quad \forall\ k \in \{\mathrm{CHP}, \mathrm{CC}\}, \quad m \in \mathrm{M}_k \tag{72}$$

$$\delta^{\text{day}}_{k,m,d,t} \leq y_{k,m,d,t} \quad \forall\ k \in \{\mathrm{CHP}, \mathrm{CC}\}, \quad m \in \mathrm{M}_k \tag{73}$$

These constraints indicate component starts within a design day. For the transition between two consecutive design days, a further set of binary variables $\delta^{\text{trans}}_{k,m,n}$ is introduced. $\delta^{\text{trans}}_{k,m,n}$ is 1 if the component is not running ($y = 0$) on the last hour of design day $\sigma(n-1)$ but is running on the first hour of the next design day $\sigma(n)$ using the assignment function $\sigma$ in Eq. (25). This way, all 365 transitions between design days are considered which is expressed by the following constraints ($\forall\ n \in \mathrm{N}_{\text{year}}:\ n \neq 1$):

$$\delta^{\text{trans}}_{k,m,n} \geq y_{k,m,\sigma(n),1} - y_{k,m,\sigma(n-1),24} \quad \forall\ k \in \{\mathrm{CHP}, \mathrm{CC}\}, \quad m \in \mathrm{M}_k \tag{74}$$

$$\delta^{\text{trans}}_{k,m,n} \leq 1 - y_{k,m,\sigma(n-1),24} \quad \forall\ k \in \{\mathrm{CHP}, \mathrm{CC}\}, \quad m \in \mathrm{M}_k \tag{75}$$

$$\delta^{\text{trans}}_{k,m,n} \leq y_{k,m,\sigma(n),1} \quad \forall\ k \in \{\mathrm{CHP}, \mathrm{CC}\}, \quad m \in \mathrm{M}_k \tag{76}$$

The cyclic condition between the last and first hour of a year is:

$$\delta^{\text{trans}}_{k,m,1} \geq y_{k,m,\sigma(1),1} - y_{k,m,\sigma(365),24} \quad \forall\ k \in \{\mathrm{CHP}, \mathrm{CC}\}, \quad m \in \mathrm{M}_k \tag{77}$$

$$\delta^{\text{trans}}_{k,m,1} \leq 1 - y_{k,m,\sigma(365),24} \quad \forall\ k \in \{\mathrm{CHP}, \mathrm{CC}\}, \quad m \in \mathrm{M}_k \tag{78}$$

$$\delta^{\text{trans}}_{k,m,1} \leq y_{k,m,\sigma(1),1} \quad \forall\ k \in \{\mathrm{CHP}, \mathrm{CC}\}, \quad m \in \mathrm{M}_k \tag{79}$$

The total start-up costs are expressed by:

$$C_{\text{starts}} = \sum_{k \in \{\text{CHP,CC}\}} \text{c}_{k,\text{start}} \sum_{m \in \text{M}_k} \left( \sum_{d \in \text{D}} \text{w}_d \sum_{t \in \text{T}} \delta^{\text{day}}_{k,m,d,t} + \sum_{n \in \text{N}_{\text{year}}} \delta^{\text{trans}}_{k,m,n} \right) \quad (80)$$

Here, $\text{c}_{k,\text{start}}$ denotes the costs per start-up. Based on cost data presented in [48], for components with a typical capacity for the EH used in the case study, the start-up costs are assumed 73.5 EUR for CHP units and 33.7 EUR for compression chillers.

### *2.3. Evaluation method and unit commitment problem*

In this section, the method for comparing and evaluating the performance of different levels of detail for MILP models is described. In the literature, a common approach to evaluate the performance of different models is to compare them to a benchmark model, which is usually the most complex model as presented in [62, 63]. In this approach, it is assumed that the model with the highest level of detail generates the most accurate results, however, this not necessarily the case [12]. In addition, the objective function values of different models cannot be compared with each other since the calculation is based on different boundary conditions: For example, a model that considers part-load efficiencies tends to have larger operational costs compared to a model which assumes constant (nominal) efficiencies. Therefore, a different evaluation method is used in this study. The method is illustrated in Fig. 3 and has also been previously used by Poncelet et al. in [8]:

In a first step, a design optimization is conducted for 24 models resulting in 24 different EH designs. In this study, an EH design describes the generation and storage capacities of all system components. The 24 models result

from different combinations of the five model features. In a second step, the operational performance of every EH design under close-to-reality conditions is determined. For this purpose, every EH design is tested in a unit commitment (UC) optimization, in which the system's operation is optimized using a detailed model which includes all five model features. The economic performance determined with the UC optimization is considered a suitable reference for the comparison of different EH designs. For each of the 24 EH designs, the UC optimization is solved in a rolling horizon scheme over an entire year. An optimization horizon of 5 days is used, which is considered a realistic forecast horizon and ensures reasonable operation of short-term storages. Based on the results, the TAC of every EH design are calculated: The TAC consist of the operational costs (gas/electricity costs, feed-in revenues, start-up costs, and maintenance costs) of all rolling horizon periods as well as annualized investments (based on the piece-wise linear investment curves). Finally, in a third step, the TAC of the UC optimization and the computing time of the design optimization are compared for all 24 models (Section 3.2).

The design optimization is solved with the commercial solver *Gurobi* (version 8) on a workstation with Intel Xeon CPU E5-2667 (2.90 GHz) and 32 GB memory. The MIP gap of the design optimization is 0.1 % and the time limit is set to 10 h (36,000 s) which is considered as a limit for usability in the planning process of energy systems. When a design optimization process is terminated due to the time limit, the best solution found to this point is used.

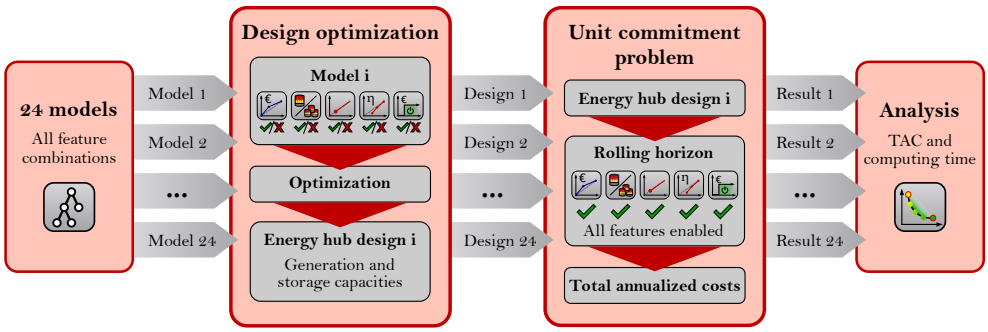


Figure 3: 24 different MILP models are evaluated in the following three-step process: Firstly, a design optimization determines the optimal EH design for each model. Secondly, the operation of all EH designs is determined for a full year in a rolling horizon scheme (unit commitment problem) and by considering all five model features. This way, the economic performance of different EH designs under realistic operational conditions are obtained. Thirdly, the computing times of the design optimization and the economic performance of the unit commitment problem are compared for all 24 models.

### *2.4. Limitations*

In this study, a detailed UC optimization is used to approximate the real operation of an EH. However, system dynamics are simplified since quasi-steady time slices with an hourly resolution are used. In addition, the UC optimization simply adopts the component capacities as they are determined in the design optimization. However, in reality only discrete components (with discrete capacities) can be installed, which would result in capacities which slightly deviate from the ones of the design optimization.

In this study, five operational model features are investigated which are expected to have the largest impact on medium-scale energy systems, like EHs for district energy systems. However, for large-scale generation units, like large fossil power plants, further operational constraints are relevant,

e.g. minimum downtimes or ramping constraints. In addition, EH designs usually have to meet the n-1 criteria since only n-1-robust designs can cover the demands even if one component fails [52]. In the design optimization in this study, the n-1 criteria is neglected and not considered as a further model feature: Firstly, considering the n-1 criteria, is highly complex and multiplies the number of additional constraints and variables which means that many models would not be solvable in a reasonable time. Secondly, the additional value of n-1 robustness can hardly be expressed in terms of TAC since it is difficult to consider component failures in the UC optimization.

A low number of design days is used in the design optimization (6 days) in order to be able to solve most of the optimization models within a reasonable time frame or, at least, achieve sufficiently low MIP gaps. However, for selected models, the optimization results have been validated with a larger number of design days and found to be consistent.

## 3. Case study

In this section, the different model formulations are applied to a use case: In Section 3.1, the use case is introduced. In the subsequent sections, the optimal system designs and their operational performances are analyzed in detail.

### *3.1. Case study description*

The case study comprises 17 buildings of a research campus in Germany. All buildings are connected to a district heating and a district cooling network. In this study, the optimal design of an EH, supplying both thermal networks, is investigated. The annual heating and cooling load profiles are

depicted in Fig. 4. The annual heat demand of the district is 6.4 GWh, and the annual cooling demand 10.0 GWh. 73 % of the cooling demand result from two data centers. The peak heat demand is 2.01 MW and the peak cold demand 2.42 MW. Heat and cold losses of both networks are estimated by static heat transfer correlations. The maximum area for PV modules is 8000 $m^2$. A detailed description of the use case is given in [64].

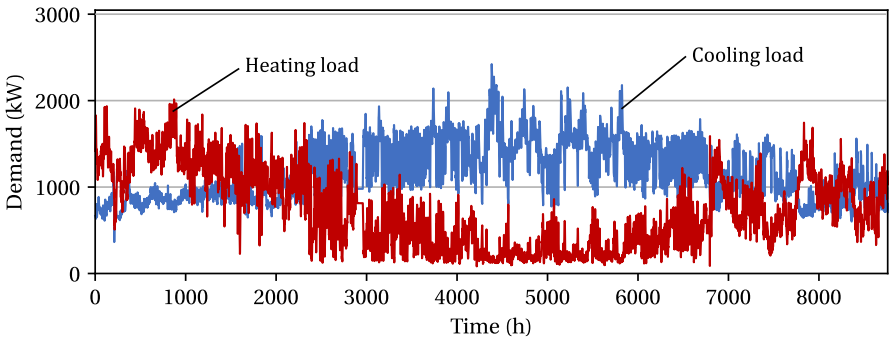


Figure 4: Load profiles of the district heating and district cooling networks.

### *3.2. Performance evaluation*

For evaluating which model is best suited for EH design optimization, the trade-off between computing time and economic performance of an EH configuration is investigated. In Fig. 5, the computing time of the design optimization as well as the TAC of the UC optimization are depicted for all 24 optimization models. A large range of the TAC between 391 and 481 kEUR/a is observed. The computing time ranges from 10 s to the time limit of 10 hours (= 36,000 s). 12 design optimizations are terminated after reaching the time limit. The MIP gap of all optimization results is listed in Table 3. Three optimizations (models 1, 2, and 9) show a MIP gap of more

than 3 % which means that the EH design of these models are uncertain and the results should be treated as such.

Models which consider part-load efficiencies in the design optimization are located in the upper left corner of Fig. 5 (low TAC, high computing times): All solutions are within the lowest 20 % of the cost range but they all reach the time limit. The model with the best performance in the UC optimization, is model 2 which considers all features except for start-up costs (`ICLE-`). The fact that model 1, which considers all features (`ICLES`), has a lower performance compared to model 2 can be explained by the remaining MIP gap of the design optimization after the time limit was reached. An extended design optimization for model 1 with an increased time limit of 48 h led to a MIP gap of 2.4 % and TAC of 392 kEUR/a.

In the bottom left corner of Fig. 5, the solutions of model 13 (`-CL-S`), 14 (`-CL--`), and 23 (`-C---`) are located. Their TAC are also within the lowest 20 % but do not include part-load efficiencies.

The models 5 (`ICL-S`), 6 (`ICL--`), and 11 (`IC---`) are located in the top right corner (high TAC, high computing time): The combination of piece-wise linear investment curves and multiple component resolution while neglecting part-load efficiencies leads to designs with large generation units but small storage units (more details in Section 3.3).

In general, it is expected that the more model features are included, the more complex the models, and the higher the expected computing time. Model 1 (`ICLES`) has the highest complexity and model 24 (`-----`) the lowest. However, results show that the computing time does not strictly correlate with the number of binary variables and SOS2 constraints which is

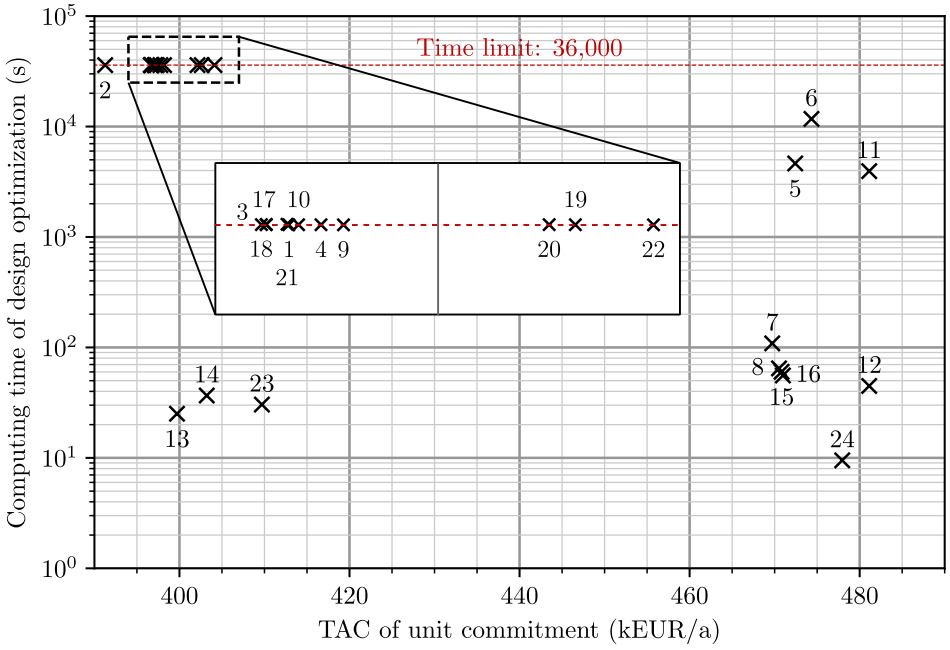


Figure 5: Trade-off between computing time of design optimization and economic performance (total annualized costs) of unit commitment problem.

Table 3: Computing time of design optimization and total annualized costs of unit commitment problem for all 24 models (MIP gap of design optimization: 0.1 %, time limit of design optimization: 36,000 s). The last column indicates the feature combination: `I`: Piece-wise linear investment curves, `C`: Multiple component resolution, `L`: Minimum part load, `E`: Part-load efficiency, `S`: Start-up costs.

| Model | Computing time (s) | MIP gap (%) | TAC (kEUR/a) | Features |
|---|---|---|---|---|
| 1 | 36,000 | 12.07 | 397 | `ICLES` |
| 2 | 36,000 | 4.03 | 391 | `ICLE-` |
| 3 | 36,000 | 0.71 | 397 | `I-LES` |
| 4 | 36,000 | 0.49 | 398 | `I-LE-` |
| 5 | 4,633 | $\leq 0.1$ | 472 | `ICL-S` |
| 6 | 11,729 | $\leq 0.1$ | 474 | `ICL--` |
| 7 | 109 | $\leq 0.1$ | 470 | `I-L-S` |
| 8 | 65 | $\leq 0.1$ | 471 | `I-L--` |
| 9 | 36,000 | 8.36 | 398 | `IC-E-` |
| 10 | 36,000 | 0.61 | 397 | `I--E-` |
| 11 | 3,945 | $\leq 0.1$ | 481 | `IC---` |
| 12 | 45 | $\leq 0.1$ | 481 | `I----` |
| 13 | 25 | $\leq 0.1$ | 400 | `-CL-S` |
| 14 | 37 | $\leq 0.1$ | 403 | `-CL--` |
| 15 | 60 | $\leq 0.1$ | 471 | `--L-S` |
| 16 | 56 | $\leq 0.1$ | 471 | `--L--` |
| 17 | 36,000 | 0.14 | 397 | `-CLES` |
| 18 | 36,000 | 1.18 | 397 | `-CLE-` |
| 19 | 36,000 | 0.64 | 403 | `--LES` |
| 20 | 36,000 | 0.92 | 402 | `--LE-` |
| 21 | 36,000 | 1.21 | 397 | `-C-E-` |
| 22 | 36,000 | 0.63 | 404 | `---E-` |
| 23 | 30 | – | 410 | `-C---` |
| 24 | 10 | – | 478 | `-----` |

in line with the findings published in [27] and indicates that the structure of constraints has a higher impact than their quantity. As described above, high computing times are observed for models which consider part-load efficiencies. Modeling part-load efficiencies adds 576 binary variables which describe in every time step the linearization of the rated capacity and the operation binary variable $y$. High computing times are also observed when both features, *piece-wise linear investments* and *multiple component resolu-*

*tion*, are considered, this is because they add 22 SOS2 constraints to the model. The features *minimum part load* and *start-up costs* do not lead to a notable increase of computing time.

### *3.3. Cost structures*

TAC consist of annualized investments as well as operational costs and revenues. The cost shares of the UC optimization are depicted for all models in Fig. 6. Natural gas purchases account for the largest and investments for the second largest share of costs. Negative costs represent revenues from the feed-in of CHP and PV power. Models with low TAC, have a higher share of investments compared to models with high TAC, which indicates that higher investments pay off over the lifetime of the energy system. For example, model 2 (`ICLE-`) has the lowest TAC (391 kEUR/a) and the share of investments is 61 % (239 kEUR/a) while model 12 (`I----`) has the highest TAC (481 kEUR/a) and the share of investments is 48 % (229 kEUR/a). The cost differences of the operational costs mainly result from gas costs (this is discussed in detail in Section 3.4.1). EH designs with high gas costs also show high electricity costs and at the same time low revenues from CHP feed-in (EH design 5-8, 11, 12, 15, 16, and 24). The share of start-up costs is negligible for all designs ($< 1\,\%$).

### *3.4. Optimal system designs*

The capacities of the conversion and storage units determined by the 24 models are depicted in Fig. 7 - 9. PV and battery capacities are not depicted since they are identical in all designs: 1.6 $\mathrm{MW_p}$ PV and no battery. Stapled columns of the same color indicate that multiple units of the same technology

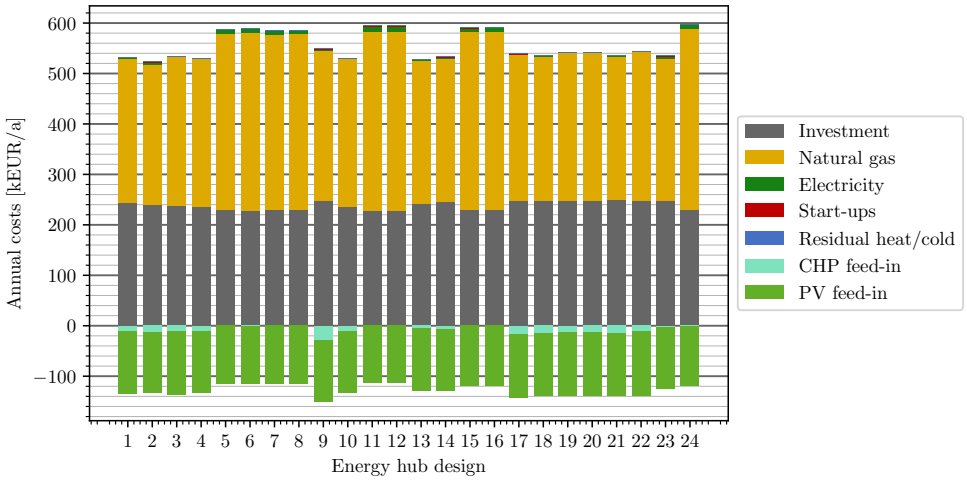


Figure 6: Shares of annual costs and revenues for all 24 energy hub designs.

are installed, e.g. in Fig. 7, design 1 comprises three gas boilers with different capacities: 0.3 MW, 0.5 MW and 0.9 MW. In addition, two CHP units are installed with a capacity of 0.08 MW and 0.15 MW. As shown in Fig. 7 and 8, the total heat and cold generation capacities are almost identical in all designs. This also results from constraints (38) and (39) which ensure that the installed capacities can meet the annual peak of heating and cooling demands and therefore ensure a minimum generation capacity. The ratio of CHP capacity to gas boiler capacity is also very similar across all designs: The total CHP capacity is about 0.25 MW and the gas boiler capacity about 1.75 MW. This means that in this case, the dimensioning of heat generation units is robust against the degree of model complexity. As depicted in Fig. 8, the dimensioning of the chillers is substantially different between the designs. In designs 19, 20, and 22, a large absorption chiller capacity of about 0.7 MW is installed, while in all other designs the absorption chiller capacity is almost

negligible ($< 0.1$ MW). The three designs with large absorption chillers also include large heat storages as they enable shifting excess heat from CHP units to times with high cooling demands. Fig. 9 depicts the capacities of heat and cold storage across all designs. The capacities substantially differ between the 24 designs: The total heat storage capacity ranges from 0.7 (EH design 24) to 4.8 MWh (EH design 3). The large differences in storage capacity result from the sizing of the generation units: A flexible generation design (with multiple small generation units) leads to smaller storages; an inflexible generation portfolio (with a single oversized generation unit) requires larger storages. This is analyzed in detail in Section 3.4.1. Cold storages are only installed in three designs: The largest cold storage (0.46 MWh) is installed in design 2. In addition, designs 18 and 21 have three small storages with a similar total capacity.

### *3.4.1. Part-load operation as cost driver*

In this section, the operation of the EH designs is analyzed in more detail. The goal is to investigate why some designs perform substantially better than others in the UC optimization. EH designs which lead to low TAC can be aggregated into three groups: The first group of designs (designs 1, 2, 9, 13, 14, 17, 18, 21, and 23) comprises multiple down-sized gas boilers and some of them multiple CHP units. The second group of designs (designs 3, 4, and 10) has large heat storage capacities and compression chillers for covering the cooling demands. A third group (designs 19, 20, and 22) has large heat storage capacities as well and in addition to compression chillers also absorption chillers.

By using either multiple small units, large storage capacities, or addi-

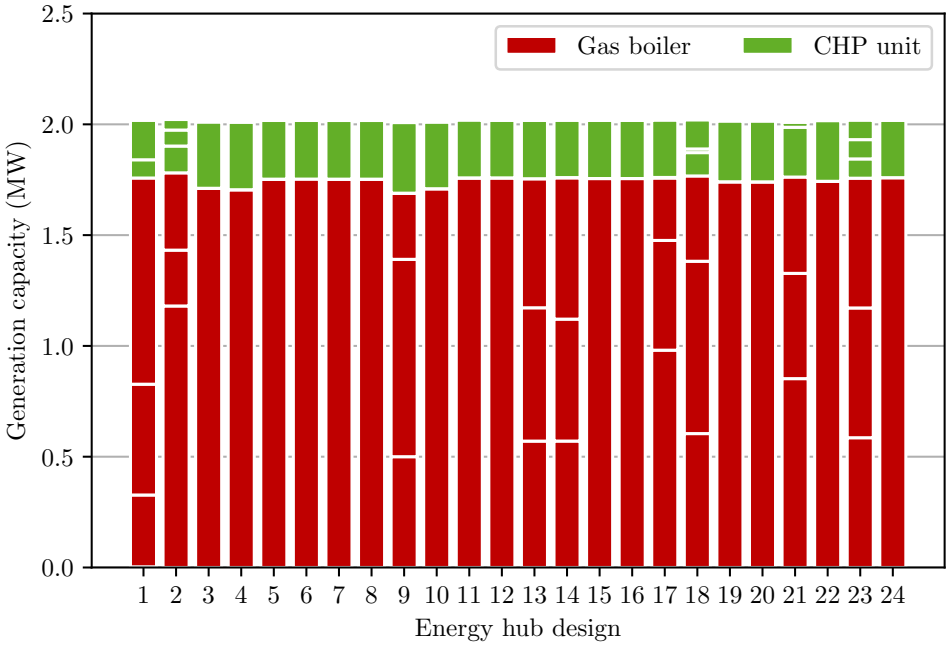


Figure 7: Installed gas boiler (nominal heating capacity) and CHP unit capacity (nominal electric power) for all 24 energy hub designs.

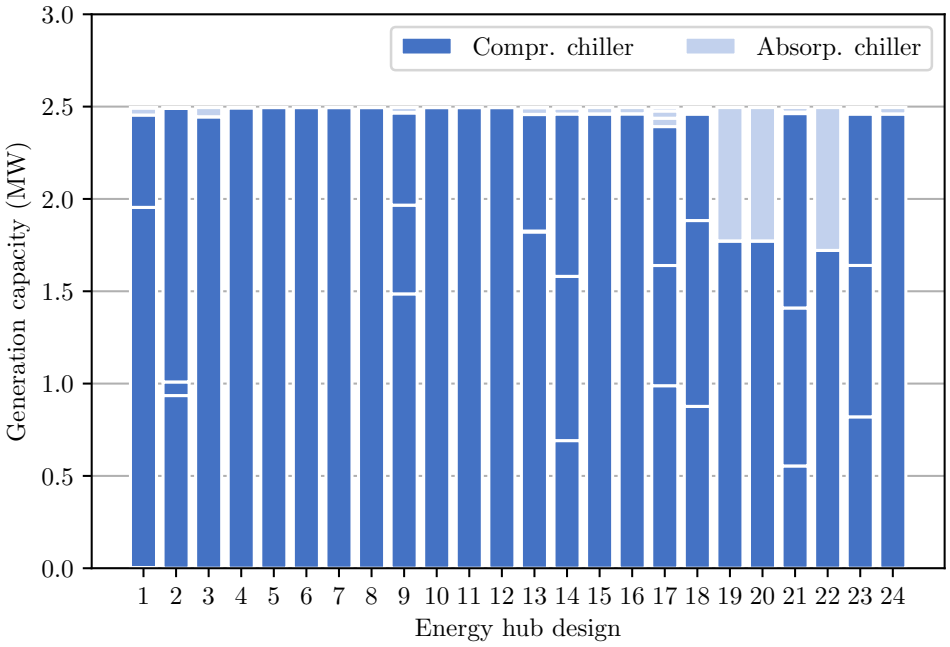


Figure 8: Installed cooling capacity of compression and absorption chillers for all 24 energy hub designs.

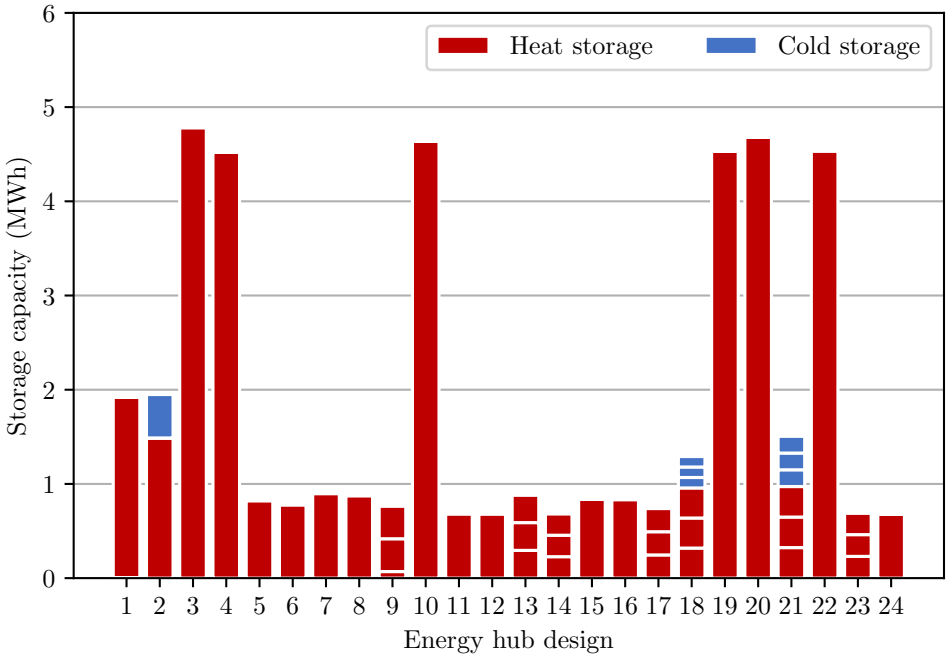


Figure 9: Installed storage capacity of heat and cold storages for all 24 energy designs.

tional absorption chillers, all designs result from maximizing the full load operation of boilers and CHP units and thus reduce part-load operation. In contrast, designs which lead to high TAC (designs 5, 6, 7, 8, 11, 12, 15, 16, and 24) comprise only one large generation unit for each technology. These units are sized with respect to peak demands and are therefore oversized during most of the year. In addition, since only small thermal storages are installed, the generation units are operated at part load most of the time. The different operation of design 4 (large unit, large storages), design 14 (multiple down-sized units, small storages), and design 11 (large unit, small storage) is depicted for a winter day in Fig. 10: In design 4, the large gas boiler is switched on multiple times a day. During operation, the gas boiler runs at full load and surplus heat is stored in the heat storage. When the gas boiler is turned off, the heat storage is discharged and covers the heat demands. In Fig 10 b), the operation of design 14 comprising three gas boilers with low capacity is depicted. A combination of two of the three gas boilers follow the heat demand profile closely and minor deviations are balanced with heat storages. The operation of EH design 11 is depicted in Fig 10 c). The design neither comprises a large heat storage nor multiple gas boilers. As a result, the large gas boiler follows the heat demand exactly which leads to substantial part-load operation and low efficiencies.

Part-load operation can be identified as a main cost driver for TAC: The cost share which fluctuates the most between the models are gas costs (Fig. 6) and therefore, since the gas price is constant over time, the gas consumption of gas boilers and CHP units has a strong impact on the costs. In addition, the ratio of boiler capacity to CHP capacity is almost the same in all EH

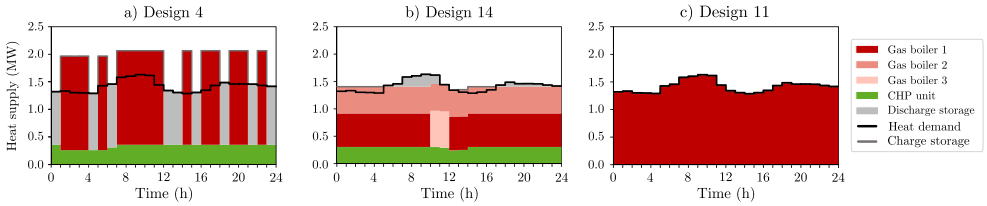


Figure 10: Heat balance for three energy hub designs on a winter day: a) Design 4 has a large heat storage capacity which enables to operate the large gas boiler at full load, switching frequently between on and off. In design 14, multiple small gas boilers ensure that the heat demand is covered at high part load. In design 11, a large gas boiler follows the demand profile exactly since no large storage units are available.

designs (c.f. Fig. 7). As a result, the fluctuations in the gas consumption result from the fact that in some EH designs, boilers and CHP units are operated at higher load, and thus at higher efficiencies. In Table 4, the share of full load operation of boilers and CHP units for four different EH designs is listed. EH design 4 and 14 have low gas costs and, in both designs, gas boilers and CHP units are operated more than 80 % of the operation time in full load. The gas boilers of design 11 and 24 are only operated in part load and CHP units operate about 80 % in part load. The full load operation of gas boilers is of particular importance: Firstly, more than half of the heat is generated by gas boilers, and secondly, the efficiency decline of gas boilers is larger than of CHP units.

## 4. Discussion

In this section, the impact of every model feature on the operational performance is discussed. Like in the previous sections, the term *model* refers to the MILP formulation and *EH design* to the corresponding system con-

Table 4: Share of annual full load operation time of gas boilers and CHP units. The high part-load operation times of boilers and CHP units in design 11 and 24 leads to increased gas consumption.

| | Design 4 | Design 11 | Design 14 | Design 24 |
|---|---|---|---|---|
| Gas boiler 1 | 0.85 | $\approx 0$ | 0.96 | $\approx 0$ |
| Gas boiler 2 | – | – | 0.94 | – |
| Gas boiler 3 | – | – | 0.85 | – |
| CHP unit 1 | 0.81 | 0.77 | 0.8 | 0.81 |
| CHP unit 2 | – | – | 1 | – |
| CHP unit 3 | – | – | 1 | – |
| Gas costs (kEUR/a) | 293.6 | 353.8 | 282.5 | 359.7 |

figuration; for example, EH design 4 is the optimal solution of model 4. As introduced in Section 3.2, the notation `ICLES` is used to describe which of the five features are considered in the respective model.

### *4.1. Piece-wise linear investment curves*

Piece-wise linear investment curves are considered in the models 1 – 12. Models 1, 2, 3, 4, 9, and 10 also include part-load efficiencies and, as described in Section 3.2, lead to low TAC and high computing times, regardless of other features. All other models (model 5, 6, 7, 8, 11, and 12) have low storage capacities and only one large component of every technology, which results in high TAC. The models 5 (`ICL-S`), 6 (`ICL--`), and 11 (`IC---`) additionally include multiple components and comprise a large number of binary variables and therefore, lead to high computing times as well.

*4.2. Multiple component resolution*

Multiple components for every technology are considered in 12 models. In 6 of these models (1, 2, 9, 17, 18, and 21) part-load efficiencies are considered, leading to high computing times and low TAC.

Models 13 (`-CL-S`) and 14 (`-CL--`) lead to an EH design with low TAC and very low computing times of 25 and 37 s, respectively. As further outlined in the following section, the features *minimum part load* (`L`) and *start-up costs* (`S`) have a small impact on the optimization. As a result, model 23 (`-C---`) shows a similar performance as models 13 and 14 with low TAC and low computing times. This is remarkable since it suggests that with a simple LP model, which models multiple components for every technology, a well-performing EH design can be obtained. In model 23, Eq. (52) ensures that the components of each technology have the same capacity in order to avoid a non-determined, random split of the total installed capacities. The total capacities of every technology in design 24 (`-----`) are almost identical to the total capacities of design 23. From this result, a simple design heuristic can be derived: Firstly, an LP model (like model 24) is solved in order to obtain the total capacities of every technology. In a second step, the total capacities are split to a defined number of components. For this heuristic, two open questions arise: At first, what is the optimal number of components that should be installed for every technology? On the one hand, an EH design with a single component for every technology lacks operational flexibility. On the other hand, a large number of components leads to unnecessary high investments due to the non-linearity of the investment curves. Secondly, since splitting the total capacity to $n$ equally sized components is

not optimal, which ratios should be used for the capacity split? For example the well-performing EH design 2 suggests to split the boiler capacity in the ratios 2.9 : 1.5 : 1. Based on the total capacities obtained with model 24, the heuristic design approach is investigated for four split ratios, as listed in Table 5: Splitting the capacity into two equally sized components, reduces the TAC from 478 kEUR/a (EH design 24) to 423 kEUR/a. A split ratio of 2:1 leads to even lower costs of 402 kEUR/a since the EH design has a larger operational flexibility. If the total capacity is split into three components, TAC of 410 kEUR/a are obtained for equally sized components (1:1:1), and 396 kEUR/a for split ratios 3:2:1.

Table 5: TAC of UC optimization based on the heuristic design approach for four split ratios with 2 and 3 components.

| Number of components | Capacity split ratio | TAC (kEUR/a) |
|---|---|---|
| 1 | No split | 478 |
| 2 | 1:1 | 423 |
| 2 | 2:1 | 402 |
| 3 | 1:1:1 | 410 |
| 3 | 3:2:1 | 396 |

### *4.3. Minimum part-load limitations*

The impact of considering minimum part load limitations (`L`) is small. This can be derived by analyzing the performance of models which only differ in this feature, e.g. models 2 (`ICLE-`) and 9 (`IC-E-`). In total, 8 of these model pairs can be identified. Since the model complexity increases when

considering minimum part load, the computing times also tend to increase, e.g. model 6 (11,729 s) compared to model 11 (3,945 s). The TAC of all model pairs are very similar: In 7 of the 8 model pairs, the model which considers minimum part load limitations has lower TAC. However, the TAC reduction lies within 2.1 % and thus, the benefit from considering minimum part load limitations is small. In 5 of 8 model pairs, the heat storage capacities are sized larger when minimum part load is considered. In two model pairs (18/24 and 14/23) the capacity is almost equal, only in one model pair (4/10), the storage capacity is smaller.

If the feature *minimum part load* is not enabled in the design optimization, small heating or cooling demands may not be covered in the UC optimization since they are lower than the minimum part load of the smallest unit. These shortages only occur in designs which are based on piece-wise linear investment curves and therefore comprise large generation capacities. The unmet heating and cooling demands are penalized by additional costs (assuming chiller COP of 6 and boiler efficiency of 0.9). However, the shortages hardly affect the results since the unmet demands are very low (0.005 % for cooling and even lower for heating). In addition, it is plausible to assume that in practice, small shortages are balanced by the thermal inertia of the generation units and the thermal networks.

### *4.4. Part-load efficiency*

As described in Section 3.4.1, part-load efficiencies have the strongest impact on the design optimization. The TAC of EH designs optimized with part-load efficiencies are all within the lowest 20 %. Models which consider part-load efficiencies lead to EH designs that ensure high full-load operation,

regardless of other model features: Multiple units are installed, even when piece-wise linear cost functions favor the installation of a single unit with large capacity (investment of multiple down-sized units is higher than one large unit). If multiple units cannot be selected, the optimization selects large storages and/or absorption chillers, which use surplus heat from boilers and CHP units. Computing times of all models with part-load efficiencies reach the time limit of 10 h.

### *4.5. Start-up costs*

In this case study, the impact of considering start-up costs (`S`) in the models is small and hardly affects the results. No remarkable difference in TAC or computing times is observed between the 7 model pairs which only differ in this feature, like the models 1 (`ICLES`) and 2 (`ICLE-`). Moreover no systematic tendencies in TAC or computing times are observed. The reasons of the low impact is that CHP units and compression chillers are operated or shut down over long time intervals and only a small number of start-ups are observed since heating and cooling demands occur mostly throughout the year. This can be different for use cases with distinct day profiles which lead to numerous start-ups and shutdowns over a year.

## 5. Conclusions and outlook

In the following sections, the main conclusions of the model analysis are summarized and an outlook on future research questions is provided.

*5.1. Conclusions*

In this paper, a systematic comparison of 24 MILP models with different levels of detail for the design of multi-energy systems is conducted. The resulting EH designs are tested in a UC optimization with high operational detail and the system performance is quantified by evaluating TAC.

The total installed generation capacities of gas boilers, CHP units, chillers, and PV modules are almost constant in all EH designs. Only in three models, the total generation capacity differs substantially (installation of more absorption chiller and less compression chiller capacity). This indicates that a simple LP model can estimate the total capacity of the technologies quite accurately. However, sizing multiple, individual components for each technology is more challenging than estimating the total capacities and the model requires a higher level of detail, especially regarding operational constraints. As a result, the TAC of the UC optimization vary widely across the models: From 391 to 481 kEUR/a (+23 %). The same applies to the computing times of the design optimization which vary from 10 s to more than 10 hours (time limit).

The analysis of the impact of the different model features lead to the following conclusions:

- The largest impact on the TAC has the share of part-load operation. As a result, a key model feature are part-load efficiencies, which in all cases lead to well performing EH designs (12 of the 14 best performing models consider part-load efficiencies). EH designs which are determined with part-load efficiencies comprise multiple components of every technology or alternatively, if multiple components are not allowed, large thermal

storages. Both, the installation of multiple small units or large thermal storages, enable a system operation in which components are operated at full load most of the time. However, considering part-load efficiencies leads to very high computing times ($>10$ hours) which is not practical for the early planning phase in which frequent updates of the boundary conditions require multiple, repetitive optimization runs.

- Models with piece-wise linear investment curves only lead to well-performing designs if part-load efficiencies are considered in the models as well (this is the case in 6 of the 9 best performing models). Otherwise, for each technology, a single oversized component and too little storage capacities are selected, which leads to high operational costs and low operational flexibility (this is the case in 6 of the 9 worst performing models).

- In the case study, minimum part-load limitations or start-up costs do not have a relevant effect on the system performance.

The model comparison shows that well-performing system designs are also obtained with LP models: Model 23, which only considers the installation of multiple components for each technology and neglects all other operational constraints in the design optimization, leads to low TAC (410 kEUR/a) and a low computation time (30 s). From this result, a simple design heuristic is derived: In a first step, an LP model is used to determine the optimal total capacity of every technology. In a second step, the total capacity is evenly distributed among several components. This hybrid approach leads to systems with low TAC while keeping computing times low as well.

*5.2. Outlook*

While this paper provides first valuable insights which model features (or feature combinations) are important in design optimization models, it also raises new questions which need to be addressed in the future:

Developing new, less complex approaches for modeling part-load efficiencies is considered a promising research path since this feature is crucial in design optimization but substantially increases the computational costs.

This study demonstrates that hybrid approaches (LP model with simple heuristics) are promising in order to determine well-performing system designs while keeping computing times small. A resulting question is how the total generation capacity (obtained from an LP) can be split to multiple components. This includes the question, how many components for each technology should be installed, and secondly, in which ratio the capacity is split. In addition, it is unclear if an LP model always determines a good approximation of the total capacity, especially with respect to storages. While this approach shows good results for the use case presented in this study, it should be applied to other use cases for further validation.

This study focuses on MILP models. However, non-linear optimization models are also widespread in energy design optimization. It would be worthwhile to conduct a similar investigation for non-linear models and investigate if non-linear models can achieve better performances than MILP models.

Besides different component models, model parameters also affect the optimal system design which leads to the following exemplary questions: What is the effect of an incorrectly assumed electricity price on the EH design and which additional costs are caused in later operation by erroneous

assumptions? Further parameters, like gas prices or the number of design days used in the design optimization, are expected to have a relevant effect on the design as well.

## 6. Acknowledgments

We gratefully acknowledge the financial support by the Federal Ministry for Economic Affairs and Energy (BMWi), promotional reference 03EWR020E (*Reallabor der Energiewende: TransUrban.NRW*).

## 7. Nomenclature

**Abbreviations**

| | |
|---|---|
| CHP | Combined heat and power |
| COP | Coefficient of performance |
| EH | Energy hub |
| LP | Linear program |
| MILP | Mixed-integer linear program |
| PV | Photovoltaics |
| SOS2 | Special Ordered Set type 2 |
| TAC | Total annualized costs |
| UC | Unit commitment |

**Indices and Sets**

| | |
|---|---|
| $d \in D$ | Design day |
| $n \in N_{\text{year}}$ | Day of year |
| $i \in N_k$ | SOS2 variable |
| $t \in T$ | Time step |
| $m \in M$ | Component |
| $k \in K$ | Technology |

**Variables**

| | |
|---|---|
| $A$ | PV area |
| $C$ | Costs |
| $\delta$ | Start-up binary variable |
| $G$ | Gas power |
| $I$ | Investment |
| $P$ | Electric power |
| $Q$ | Thermal power |
| $R$ | Revenue |
| $S$ | State of charge |
| $y$ | On/off binary variable |
| $\xi$ | SOS2 auxiliary variable |
| $cap$ | Generation/storage capacity |

**Parameters**

| | |
|---|---|
| a | Annuity factor |
| $\beta$ | Heat ratio |
| c | Start-up costs |
| $\eta$ | Efficiency |
| f | Operation & maintenance factor |
| G | Solar irradiance |
| i | Specific investment |
| $\hat{\mathrm{M}}$ | Big-M coefficient |
| p | Energy supply price |
| PLR | Part-load ratio |
| r | Feed-in tariff |
| $\tau$ | Minimum (dis-)charging time |
| $\mathrm{w_d}$ | Design day weight |
| $\phi$ | Storage loss factor |
| $\lambda$ | Part-load parameter |
| $\gamma$ | Part-load parameter |

**Sub- and superscripts**

| | |
|---|---|
| AC | absorption chiller |
| aux | auxiliary |
| BAT | battery |
| BOI | boiler |
| c | cooling |
| cap | capacity |
| CC | compression chiller |
| ch/dch | charge/discharge |
| CHP | combined heat and power |
| CTES | cold thermal energy storage |
| dem | demand |
| el | electricity |
| feed-in | electricity feed-in |
| gas | natural gas |
| grid | electricity grid |
| h | heating |
| inv | investment |
| loss | thermal loss |
| max | maximum |
| min | minimum |
| nom | nominal |
| om | operation & maintenance |
| STC | Standard Test Conditions |
| starts | component starts |
| sto | storage |
| sol | solar |
| TES | thermal energy storage |
| tot | total |
| trans | transition |

## Appendix A. Model parameters

Table A.6 lists the economic parameters of generation and storage technologies. In Table A.7, further general model parameters are listed.

Table A.6: Economic parameters of technologies.

| | Gas Boiler | CHP unit | Comp. chiller | Absorp. chiller | PV | Thermal Storage | Battery |
|---|---|---|---|---|---|---|---|
| Life time [a] | 20 | 15 | 15 | 18 | 20 | 20 | 10 |
| Annuity factor $a_{inv}$ [%] | 8.02 | 9.87 | 9.87 | 8.67 | 8.02 | 8.02 | 12.95 |
| Share op. & main. $f_{om}$ [%] | 3 | 8 | 3.5 | 3 | 1 | 2 | 1 |

Table A.7: General model parameters.

| Parameter | Value |
|---|---|
| $p_{gas}$ | 0.028 EUR/kWh |
| $G_{sol,STC}$ | 1000 W/m$^2$ |
| $\eta_{PV,STC}$ | 20.8 % |
| $\eta^{nom}_{el,CHP}$ | 40.5 % |
| $\eta^{nom}_{th,CHP}$ | 47.8 % |
| $\eta^{nom}_{BOI}$ | 90 % |
| $COP^{nom}_{CC}$ | 6 |
| $\beta^{nom}_{AC}$ | 68 % |

### *Appendix A.1. Investment curves*

The linear and piece-wise linear fits of investments are depicted in Fig. A.11−A.15.

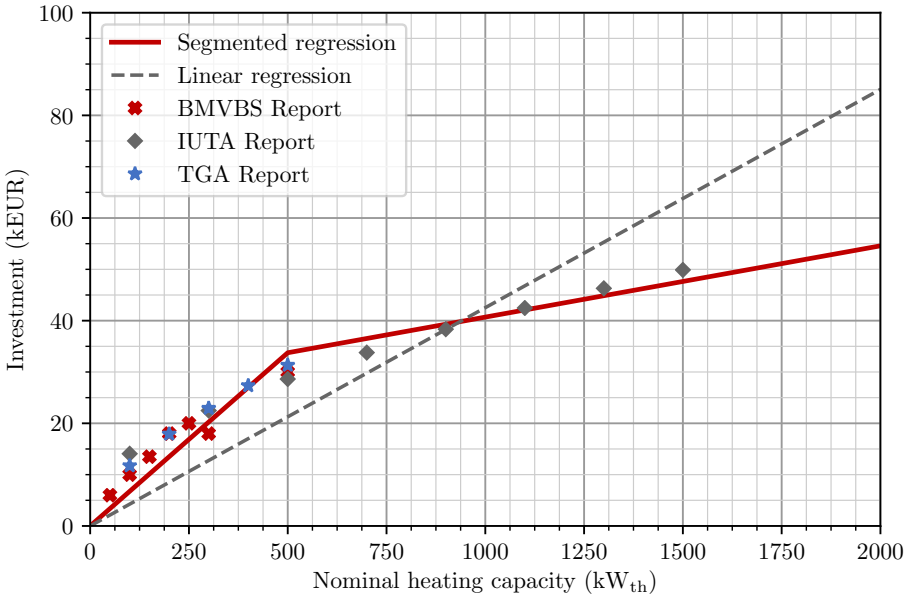


Figure A.11: Linear and piece-wise linear fit of gas boiler investment based on [65, 66, 67].

*Appendix A.2. Part-load efficiencies*

The linearization parameters used for modeling part-load efficiencies are listed in Table A.8. A comparison of the linearized and non-linear efficiency curves are depicted in Fig. A.16 and the linearization method is visualized in Fig. A.17. The numeric values of part-load efficiency curves are listed in Tables A.9 to A.12.

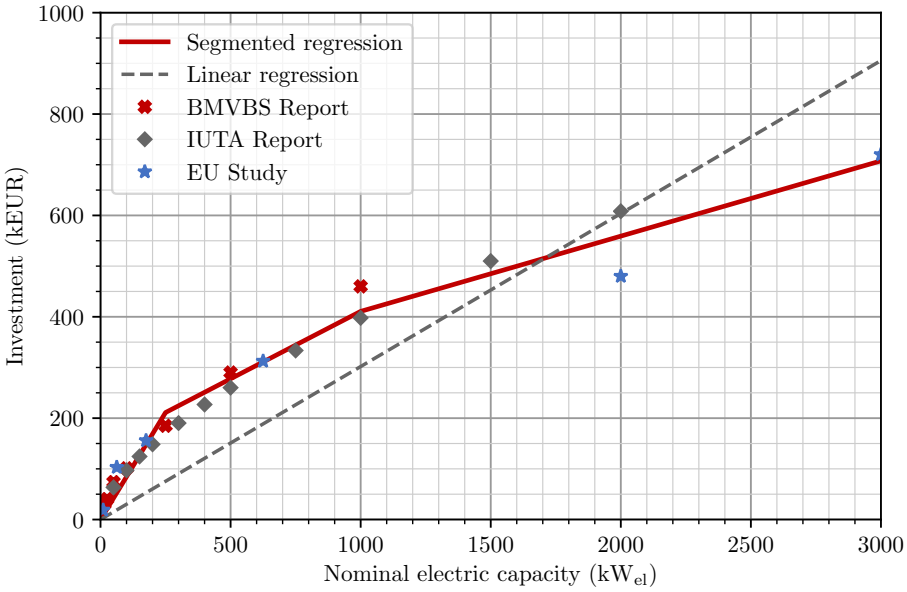


Figure A.12: Linear and piece-wise linear fit of CHP unit investment based on [65, 67, 68].

Table A.8: Parameters $\gamma$ and $\lambda$ for the linearization of part-load efficiencies.

| | $\gamma$ | $\lambda$ |
|---|---|---|
| Gas boiler | 0.4576 | 0.6599 |
| CHP unit (el) | 0.2548 | 2.2135 |
| CHP unit (th) | 0.2244 | 0.9545 |
| Compr. chiller | 0.0435 | 0.1189 |
| Absorp. chiller | 0.0510 | 1.3565 |

Table A.9: Part-load efficiency of gas boilers [71]

| PLR | 1 | 0.9 | 0.8 | 0.7 | 0.6 | 0.5 | 0.4 | 0.3 | 0.2 |
|---|---|---|---|---|---|---|---|---|---|
| $\eta_{BOI}$ | 0.9 | 0.86 | 0.81 | 0.76 | 0.70 | 0.62 | 0.56 | 0.45 | 0.35 |

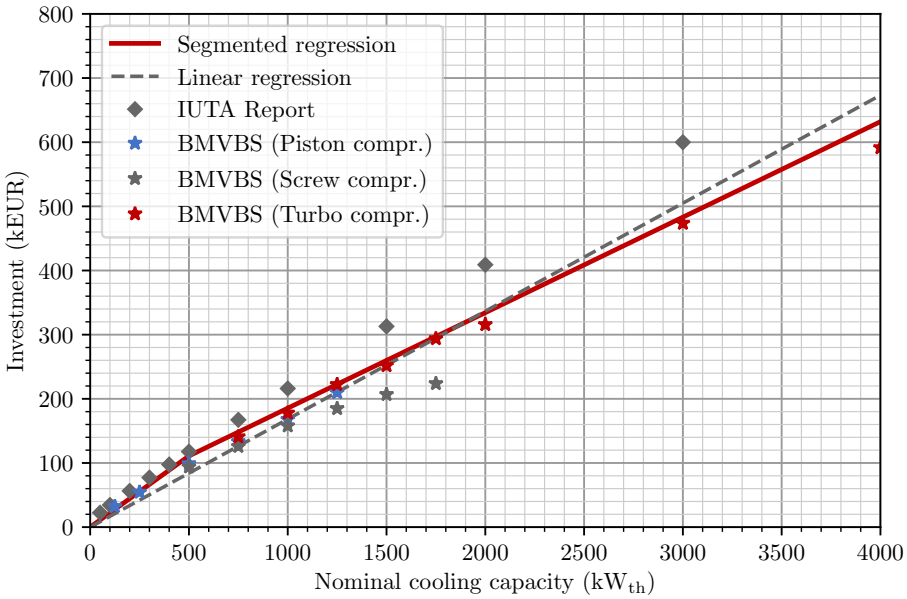


Figure A.13: Linear and piece-wise linear fit of compression chiller investment based on [65, 67].

Table A.10: Part-load efficiency of CHP units [72]

| PLR | 1 | 0.75 | 0.5 |
|---|---|---|---|
| $\eta_{\mathrm{BHKW,el}}$ | 0.405 | 0.392 | 0.367 |
| $\eta_{\mathrm{BHKW,th}}$ | 0.478 | 0.49 | 0.516 |

Table A.11: Part-load efficiency of compression chillers [73]

| $PLR$ | 1 | 0.92 | 0.84 | 0.74 | 0.68 | 0.58 | 0.50 | 0.42 | 0.34 | 0.26 |
|---|---|---|---|---|---|---|---|---|---|---|
| $COP_{\mathrm{CC}}$ | 5.74 | 5.92 | 6 | 5.92 | 5.73 | 5.48 | 5.05 | 4.61 | 3.95 | 3.04 |

Table A.12: Part-load efficiency of absorption chillers [71]

| PLR | 1 | 0.9 | 0.8 | 0.7 | 0.6 | 0.5 | 0.4 | 0.3 | 0.2 |
|---|---|---|---|---|---|---|---|---|---|
| $\beta_{\mathrm{AC}}$ | 0.68 | 0.71 | 0.72 | 0.73 | 0.71 | 0.79 | 0.67 | 0.63 | 0.56 |

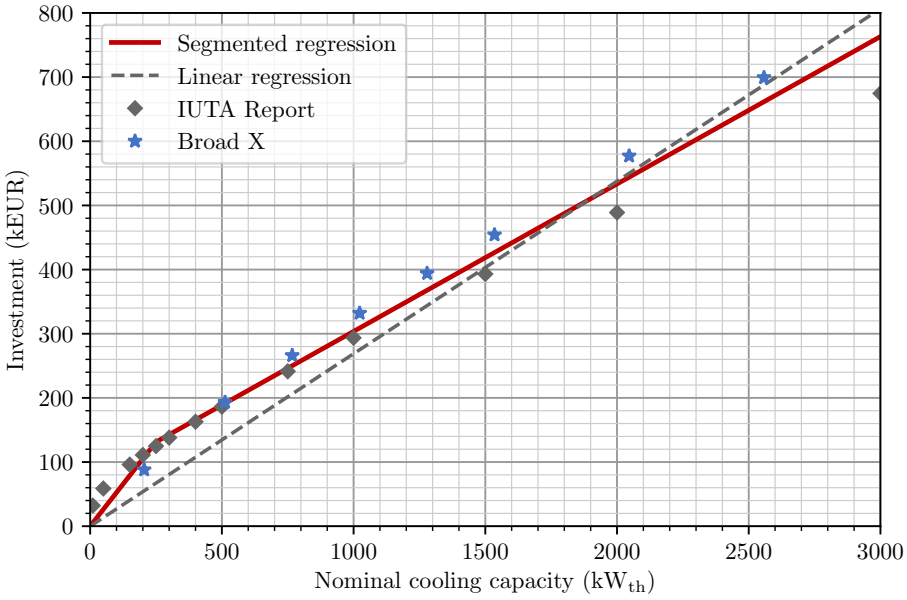


Figure A.14: Linear and piece-wise linear fit of absorption chiller investment based on [65, 69].

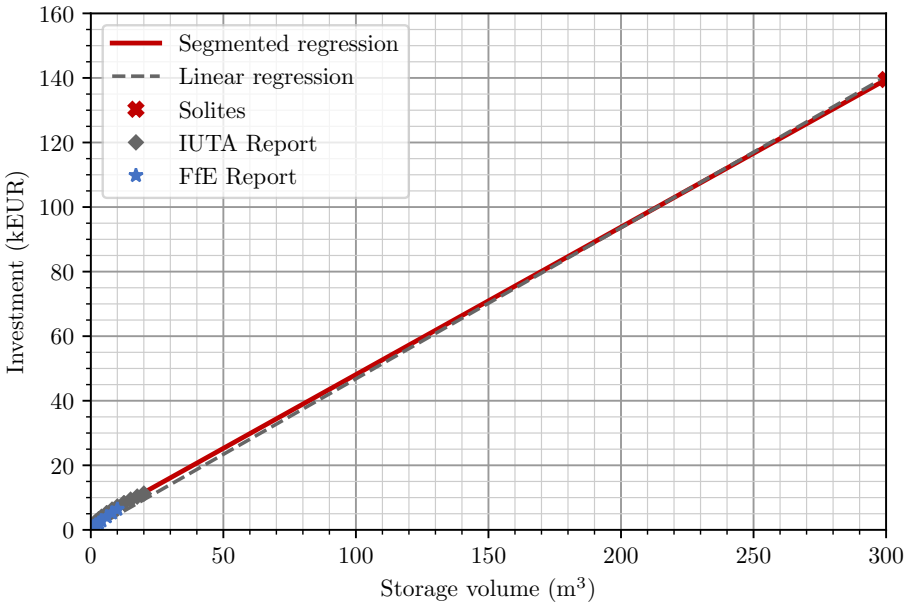


Figure A.15: Linear and piece-wise linear fit of thermal energy storage investment based on [65, 70].

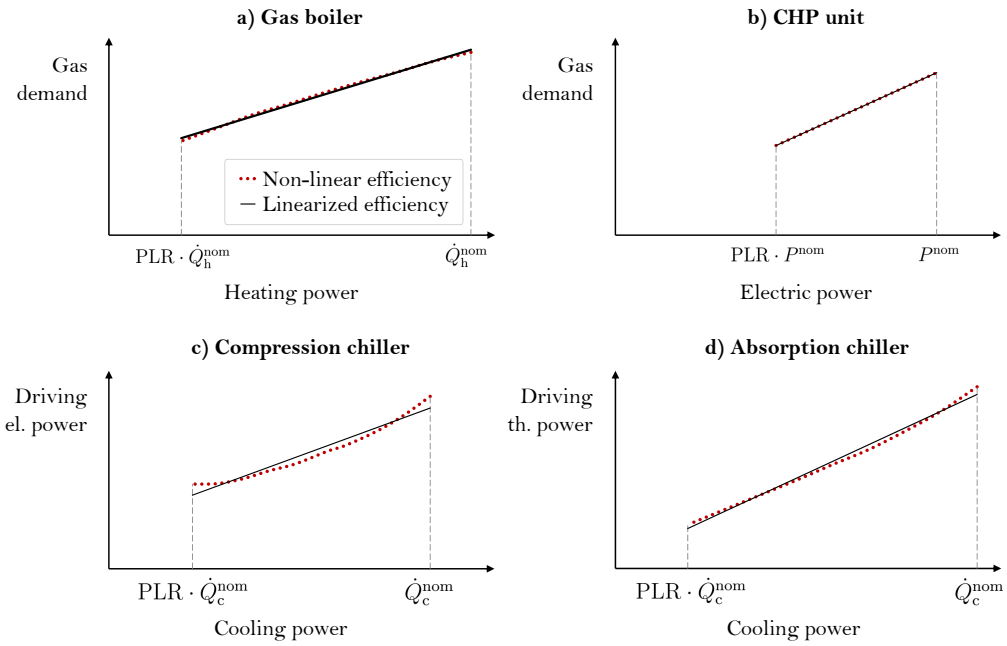


Figure A.16: Non-linear (red) and linearized (black) efficiency curve of gas boiler, CHP unit, compression and absorption chiller. The vertical axis describes the input power (gas, electricity, heat), the horizontal axis the output power (heat, electricity, cold). The efficiency curves are modeled between the minimum part-load ratio (PLR) and the nominal capacity.

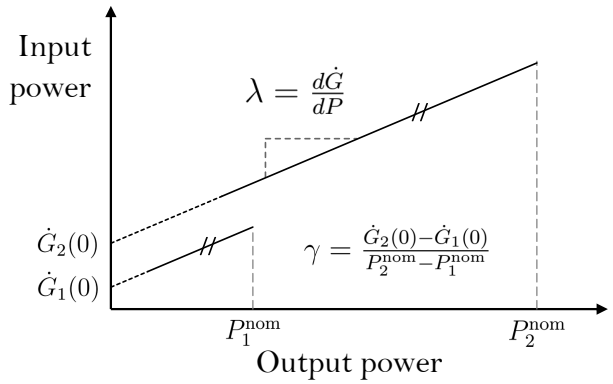


Figure A.17: The parameter $\gamma$ describes the change of the offset of the linearized function when changing the rated power. $\lambda$ is the slope of the linear function.

## References


[1] H. Lund, N. Duic, P. A. Østergaard, B. V. Mathiesen, Future district heating systems and technologies: On the role of smart energy systems and 4th generation district heating, Energy 165 (2018) 614–619 (2018). doi:10.1016/j.energy.2018.09.115.

[2] P. Mancarella, MES (multi-energy systems): An overview of concepts and evaluation models, Energy 65 (2014) 1–17 (2014). doi:10.1016/j.energy.2013.10.041.

[3] G. Mavromatidis, K. Orehounig, J. Carmeliet, Design of distributed energy systems under uncertainty: A two-stage stochastic programming approach, Applied Energy 222 (2018) 932–950 (2018). doi:10.1016/j.apenergy.2018.04.019.

[4] G. Mavromatidis, K. Orehounig, L. A. Bollinger, M. Hohmann, J. F. Marquant, S. Miglani, B. Morvaj, P. Murray, C. Waibel, D. Wang, J. Carmeliet, Ten questions concerning modeling of distributed multi-energy systems, Building and Environment 165 (2019) 106372 (2019). doi:10.1016/j.buildenv.2019.106372.

[5] M. Sameti, F. Haghighat, Optimization approaches in district heating and cooling thermal network, Energy and Buildings 140 (2017) 121–130 (2017). doi:10.1016/j.enbuild.2017.01.062.

[6] E. Cuisinier, C. Bourasseau, A. Ruby, P. Lemaire, B. Penz, Techno-economic planning of local energy systems through optimization models: a survey of current methods, International Journal of Energy Research

45 (4) (2021) 4888–4931 (2021). doi:https://doi.org/10.1002/er.6208.

[7] D. P. Schlachtberger, T. Brown, M. Schäfer, S. Schramm, M. Greiner, Cost optimal scenarios of a future highly renewable European electricity system: Exploring the influence of weather data, cost parameters and policy constraints, Energy 163 (2018) 100–114 (2018). doi:10.1016/j.energy.2018.08.070.

[8] K. Poncelet, E. Delarue, D. Six, J. Duerinck, W. D'haeseleer, Impact of the level of temporal and operational detail in energy-system planning models, Applied Energy 162 (2016) 631–643 (2016). doi:10.1016/j.apenergy.2015.10.100.

[9] L. Nolting, A. Praktiknjo, Is the more complex model always the better one? Evidence from the assessment of security of electricity supply, ENERDAY 2019 – The 13th International Conference on Energy Economics and Technology (2019). doi:10.13140/RG.2.2.32770.63684.

[10] A. Pollok, D. Bender, Using multi-objective optimization to balance system-level model complexity, in: P. Pepper, D. Broman (Eds.), Proceedings of the 6th International Workshop on Equation-Based Object-Oriented Modeling Languages and Tools, ACM, New York, NY, 2014, pp. 69–78 (2014). doi:10.1145/2666202.2666213.

[11] E. Ridha, L. Nolting, A. Praktiknjo, Complexity profiles: A large-scale review of energy system models in terms of complexity, Energy Strategy Reviews (30) (2020). doi:10.1016/j.esr.2020.100515.

[12] R. Orth, M. Staudinger, S. I. Seneviratne, J. Seibert, M. Zappa, Does model performance improve with complexity? A case study with three hydrological models, Journal of Hydrology (523) (2015) 147–159 (2015). doi:10.1016/j.jhydrol.2015.01.044.

[13] S. Winkelmüller, Optimierung der Nachfrage-und Erzeugungsstruktur kommunaler Energiesysteme am Beispiel von Wien, Augsburg: Institut für Physik, Universität Augsburg (2006).

[14] C. Senkpiel, Akteursverhalten und -strukturen in der Energiesystemanalyse (Actor behavior and structures in energy system analysis), Presentation at the Workshop on Complexity in Energy System Analysis, Meeting of the German Research Network on Energy Systems, Berlin, Germany (2018).

[15] S. Simoes, M. Zeyringer, D. Mayr, T. Huld, W. Nijs, J. Schmidt, Impact of different levels of geographical disaggregation of wind and PV electricity generation in large energy system models: A case study for Austria, Renewable Energy (105) (2017) 183–198 (2017).

[16] L. Kotzur, P. Markewitz, M. Robinius, D. Stolten, Impact of different time series aggregation methods on optimal energy system design, Renewable Energy 117 (2018) 474–487 (2018). doi:10.1016/j.renene.2017.10.017.

[17] J. F. Marquant, G. Mavromatidis, R. Evins, J. Carmeliet, Comparing different temporal dimension representations in distributed energy

system design models, Energy Procedia 122 (2017) 907–912 (2017). doi:10.1016/j.egypro.2017.07.403.

[18] S. Babrowski, T. Heffels, P. Jochem, W. Fichtner, Reducing computing time of energy system models by a myopic approach, Energy systems (5) (2014) 65–83 (2014).

[19] T. Ommen, W. B. Markussen, B. Elmegaard, Comparison of linear, mixed integer and non-linear programming methods in energy system dispatch modelling, Energy (74) (2014) 109–118 (2014).

[20] D. Putz, D. Schwabeneder, H. Auer, B. Fina, A comparison between mixed-integer linear programming and dynamic programming with state prediction as novelty for solving unit commitment, International Journal of Electrical Power & Energy Systems 125 (2021) 106426 (2021). doi:10.1016/j.ijepes.2020.106426.

[21] M. Welsch, P. Deane, M. Howells, B. Ó Gallachóir, F. Rogan, M. Bazilian, H.-H. Rogner, Incorporating flexibility requirements into long-term energy system models – A case study on high levels of renewable electricity penetration in Ireland, Applied Energy 135 (2014) 600–615 (2014). doi:10.1016/j.apenergy.2014.08.072.

[22] H. C. Gils, T. Pregger, F. Flachsbarth, M. Jentsch, C. Dierstein, Comparison of spatially and temporally resolved energy system models with a focus on Germany's future power supply, Applied Energy (255) (2019).

[23] P. Gabrielli, M. Gazzani, M. Mazzotti, Electrochemical conversion technologies for optimal design of decentralized multi-energy systems: Mod-

eling framework and technology assessment, Applied Energy 221 (2018) 557–575 (2018). doi:10.1016/j.apenergy.2018.03.149.

[24] Z. Zhou, P. Liu, Z. Li, E. N. Pistikopoulos, M. C. Georgiadis, Impacts of equipment off-design characteristics on the optimal design and operation of combined cooling, heating and power systems, Computers & Chemical Engineering 48 (2013) 40–47 (2013). doi:10.1016/j.compchemeng.2012.08.007.

[25] B. Palmintier, M. Webster, Impact of unit commitment constraints on generation expansion planning with renewables, IEEE Power and Energy Society General Meeting 2011, 24.07.2011 - 29.07.2011, pp. 1–7 (24.07.2011 - 29.07.2011). doi:10.1109/PES.2011.6038963.

[26] N. Helistö, J. Kiviluoma, G. Morales-España, C. O'Dwyer, Impact of operational details and temporal representations on investment planning in energy systems dominated by wind and solar, Applied Energy 290 (2021) 116712 (2021). doi:10.1016/j.apenergy.2021.116712.

[27] R. Evins, K. Orehounig, V. Dorer, J. Carmeliet, New formulations of the 'energy hub' model to address operational constraints, Energy 73 (2014) 387–398 (2014). doi:10.1016/j.energy.2014.06.029.

[28] R. Yokoyama, K. Ito, Optimal design of energy supply systems based on relative robustness criterion, Energy Conversion and Management 43 (4) (2002) 499–514 (2002). doi:10.1016/S0196-8904(01)00027-9.

[29] C. Weber, N. Shah, Optimisation based design of a district energy sys-

tem for an eco-town in the United Kingdom, Energy 36 (2) (2011) 1292–1308 (2011). doi:10.1016/j.energy.2010.11.014.

[30] S. Fazlollahi, P. Mandel, G. Becker, F. Maréchal, Methods for multi-objective investment and operating optimization of complex energy systems, Energy 2012 (45) (2012) 12–22 (2012).

[31] P. Voll, C. Klaffke, M. Hennen, S. Kirschbaum, A. Bardow, Synthesis and Optimization of Distributed Energy Supply Systems using Automated Superstructure and Model Generation, in: I. A. Karimi, R. Srinivasan (Eds.), Computer Aided Chemical Engineering : 11 International Symposium on Process Systems Engineering, Vol. 31, Elsevier, 2012, pp. 1712–1716 (2012). doi:10.1016/B978-0-444-59506-5.50173-5.

[32] A. Omu, R. Choudhary, A. Boies, Distributed energy resource system optimisation using mixed integer linear programming, Energy Policy 61 (2013) 249–266 (2013). doi:10.1016/j.enpol.2013.05.009.

[33] K. A. Pruitt, R. J. Braun, A. M. Newman, Evaluating shortfalls in mixed-integer programming approaches for the optimal design and dispatch of distributed generation systems, Applied Energy 102 (2013) 386–398 (2013). doi:10.1016/j.apenergy.2012.07.030.

[34] P. Voll, Automated optimization-based synthesis of distributed energy supply systems: Zugl.: Aachen, Techn. Hochsch., Diss., 2013, 1st Edition, Vol. 1 of Aachener Beiträge zur Technischen Thermodynamik, Wissenschaftsverl. Mainz, Aachen, 2014 (2014).

[35] T. Wakui, R. Yokoyama, Optimal structural design of residential cogeneration systems in consideration of their operating restrictions, Energy 64 (2014) 719–733 (2014). doi:10.1016/j.energy.2013.10.002.

[36] A. Bischi, L. Taccari, E. Martelli, E. Amaldi, G. Manzolini, P. Silva, S. Campanari, E. Macchi, A detailed MILP optimization model for combined cooling, heat and power system operation planning, Energy 74 (2014) 12–26 (2014). doi:10.1016/j.energy.2014.02.042.

[37] A. Rieder, A. Christidis, G. Tsatsaronis, Multi criteria dynamic design optimization of a small scale distributed energy system, Energy 74 (2014) 230–239 (2014). doi:10.1016/j.energy.2014.06.007.

[38] R. Yokoyama, Y. Shinano, S. Taniguchi, M. Ohkura, T. Wakui, Optimization of energy supply systems by MILP branch and bound method in consideration of hierarchical relationship between design and operation, Energy Conversion and Management 92 (2015) 92–104 (2015). doi:10.1016/j.enconman.2014.12.020.

[39] Y. Yang, S. Zhang, Y. Xiao, Optimal design of distributed energy resource systems coupled with energy distribution networks, Energy 85 (2015) 433–448 (2015). doi:10.1016/j.energy.2015.03.101.

[40] C. Milan, M. Stadler, G. Cardoso, S. Mashayekh, Modeling of non-linear CHP efficiency curves in distributed energy systems, Applied Energy 148 (2015) 334–347 (2015). doi:10.1016/j.apenergy.2015.03.053.

[41] K. Akbari, F. Jolai, S. F. Ghaderi, Optimal design of distributed energy

system in a neighborhood under uncertainty, Energy 116 (2016) 567–582 (2016). doi:10.1016/j.energy.2016.09.083.

[42] B. Morvaj, R. Evins, J. Carmeliet, Optimising urban energy systems: Simultaneous system sizing, operation and district heating network layout, Energy 116 (2016) 619–636 (2016). doi:10.1016/j.energy.2016.09.139.

[43] M. Li, H. Mu, N. Li, B. Ma, Optimal design and operation strategy for integrated evaluation of CCHP (combined cooling heating and power) system, Energy 99 (2016) 202–220 (2016). doi:10.1016/j.energy.2016.01.060.

[44] S. Goderbauer, B. Bahl, P. Voll, M. E. Lübbecke, A. Bardow, A. M. Koster, An adaptive discretization MINLP algorithm for optimal synthesis of decentralized energy supply systems, Computers & Chemical Engineering (95) (2016) 38–48 (2016).

[45] D. E. Majewski, M. Wirtz, M. Lampe, A. Bardow, Robust multi-objective optimization for sustainable design of distributed energy supply systems, Computers & Chemical Engineering 102 (2017) 26–39 (2017). doi:10.1016/j.compchemeng.2016.11.038.

[46] S. Deng, Q. Wu, Z. Jing, L. Wu, F. Wei, X. Zhou, Optimal Capacity Configuration for Energy Hubs Considering Part-Load Characteristics of Generation Units, Energies 10 (12) (2017) 1966 (2017). doi:10.3390/en10121966.

[47] T. Schütz, M. H. Schraven, S. Remy, J. Granacher, D. Kemetmüller, M. Fuchs, D. Müller, Optimal design of energy conversion units for residential buildings considering German market conditions, Energy 139 (2017) 895–915 (2017). doi:10.1016/j.energy.2017.08.024.

[48] A. Dolatabadi, B. Mohammadi-Ivatloo, Stochastic risk-constrained scheduling of smart energy hub in the presence of wind power and demand response, Applied Thermal Engineering 123 (2017) 40–49 (2017). doi:10.1016/j.applthermaleng.2017.05.069.

[49] R. Jing, X. Zhu, Z. Zhu, W. Wang, C. Meng, N. Shah, N. Li, Y. Zhao, A multi-objective optimization and multi-criteria evaluation integrated framework for distributed energy system optimal planning, Energy Conversion and Management 166 (2018) 445–462 (2018). doi:10.1016/j.enconman.2018.04.054.

[50] A. Gonzalez-Castellanos, P. G. Thakurta, A. Bischi, Flexible unit commitment of a network-constrained combined heat and power system. URL http://arxiv.org/pdf/1809.09508v1

[51] M. Karmellos, G. Mavrotas, Multi-objective optimization and comparison framework for the design of Distributed Energy Systems, Energy Conversion and Management 180 (2019) 473–495 (2019). doi:10.1016/j.enconman.2018.10.083.

[52] D. E. Hollermann, D. F. Hoffrogge, F. Mayer, M. Hennen, A. Bardow, Optimal ( n−1 )-reliable design of distributed energy supply systems,

Computers & Chemical Engineering 121 (2019) 317–326 (2019). doi:10.1016/j.compchemeng.2018.09.029.

[53] R. K. Ellsworth, Capacity Factor Cost Modeling for Gas-Fired Power Plants, Construction Accounting & Taxation 19 (1) (2009) 31 (2009).

[54] L. R. Dysert, Sharpen your cost estimating skills, Cost Engineering 45 (6) (2003) 22 (2003).

[55] Energinet.dk, SIFRE: Simulation of Flexible and Renewable Energy sources (2016) 1–34 (2016).

[56] P. Voll, M. Jennings, M. Hennen, N. Shah, A. Bardow, The optimum is not enough: A near-optimal solution paradigm for energy systems synthesis, Energy 82 (2015) 446–456 (2015). doi:10.1016/j.energy.2015.01.055.

[57] T. Schütz, M. H. Schraven, M. Fuchs, P. Remmen, D. Müller, Comparison of clustering algorithms for the selection of typical demand days for energy system synthesis, Renewable Energy 129 (2018) 570–582 (2018). doi:10.1016/j.renene.2018.06.028.

[58] F. Domínguez-Muñoz, J. M. Cejudo-López, A. Carrillo-Andrés, M. Gallardo-Salazar, Selection of typical demand days for CHP optimization, Energy and Buildings 43 (11) (2011) 3036–3043 (2011). doi:10.1016/j.enbuild.2011.07.024.

[59] IEC System of Conformity Assessment Schemes for Electrotechnical Equipment and Components, IEC 61215. Terrestrial photovoltaic (PV) modules - Design qualification and type approval. (2016).

[60] P. Gabrielli, M. Gazzani, E. Martelli, M. Mazzotti, Optimal design of multi-energy systems with seasonal storage, Applied Energy 219 (2018) 408–424 (2018). doi:10.1016/j.apenergy.2017.07.142.

[61] L. Kotzur, P. Markewitz, M. Robinius, D. Stolten, Time series aggregation for energy system design: Modeling seasonal storage, Applied Energy 213 (2018) 123–135 (2018). doi:10.1016/j.apenergy.2018.01.023.

[62] J. Priesmann, L. Nolting, A. Praktiknjo, Are complex energy system models more accurate? An intra-model comparison of power system optimization models, Applied Energy 255 (2019) 113783 (2019). doi:10.1016/j.apenergy.2019.113783.

[63] T. Schütz, R. Streblow, D. Müller, A comparison of thermal energy storage models for building energy system optimization, Energy and Buildings 93 (2015) 23–31 (2015). doi:10.1016/j.enbuild.2015.02.031.

[64] M. Wirtz, L. Kivilip, P. Remmen, D. Müller, 5th Generation District Heating: A novel design approach based on mathematical optimization, Applied Energy 260 (2020) 114158 (2020). doi:10.1016/j.apenergy.2019.114158.

[65] M. Gebhardt, H. Kohl, T. Steinrötter, Preisatlas: Ableitung von Kostenfunktionen für Komponenten der rationellen Energienutzung. Institut für Energie- und Umwelttechnik e.V.
URL https://vdocuments.net/preisatlas.html

[66] K. Jagnow, I. Sell, D. Wolff, Investitionskostenfunktionen TGA.
URL https://www.delta-q.de/export/sites/default/de/downloads/investitionskosten_tga_1.pdf

[67] A. Hempel, H. P. Schettler-Köhler, A. Vilz, D. Thiel, M. Ehrlich, Ermittlung von spezifischen Kosten energiesparender Bauteil-, Beleuchtungs-, Heizungs- und Klimatechnikausführungen bei Nichtwohngebäuden für die Wirtschaftlichkeitsuntersuchungen zur EnEV 2012. Bundesministerium für Verkehr, Bau und Stadtentwicklung.
URL https://www.bbsr.bund.de/BBSR/DE/veroeffentlichungen/ministerien/bmvbs/bmvbs-online/2012/ON082012.html?nn=423048

[68] T. Fleiter, J. Steinbach, M. Ragwitz, Mapping and analyses of the current and future (2020 - 2030) heating/cooling fuel deployment (fossil/renewables). European Commission Directorate C. 2 – New energy technologies, innovation and clean coal.

[69] BROAD X. Absorption Chiller: Model Selection & Design Manual. 2018.

[70] F. Samweber, C. Schifflechner, Kostenanalyse Wärmespeicher bis 10.000l Speichergröße. Forschungsstelle für Energiewirtschaft e.V.
URL https://www.ffe.de/publikationen/veroeffentlichungen/659-kostenanalyse-waermespeicher-bis-10-000-l-speichergroesse

[71] P. Liu, M. C. Georgiadis, E. N. Pistikopoulos, An energy systems engineering approach for the design and operation of microgrids in residential applications, Chemical Engineering Research and Design 91 (10) (2013) 2054–2069 (2013). doi:10.1016/j.cherd.2013.08.016.

[72] GE Jenbacher GmbH & Co OHG, Technical Specification: JMS 312 GS-N.L. (2020).

[73] F. W. Yu, K. T. Chan, Part load performance of air-cooled centrifugal chillers with variable speed condenser fan control, Building and Environment 42 (11) (2007) 3816–3829 (2007). doi:10.1016/j.buildenv.2006.11.029.